The Rosenzweig-Macarthur Graphical Criterion for a Predator-Prey Model with Variable Mortality Rate

Amina Hammoum, Tewfik Sari, Karim Yadi

THE ROSENZWEIG-MACARTHUR GRAPHICAL CRITERION FOR A PREDATOR-PREY MODEL WITH VARIABLE MORTALITY RATE

AMINA HAMMOUM, TEWFIK SARI, AND KARIM YADI

Abstract. We consider a general modified Gause type model of predation, for which the predator mortality rate can depend on the densities of both species, prey and predator. We give a graphical criterion for the stability of positive hyperbolic equilibria, which is an extension of the well-known Rosenzweig-MacArthur graphical criterion for the case of a constant predator mortality rate. We examine the occurrence of a Poincaré-Andronov-Hopf bifurcation and give an expression for the first Lyapunov coefficient. Our model generalizes several models appearing in the literature. The relevance of our results, i.e. the use of the graphical criterion and the expression for the first Lyapunov coefficient, is tested on these models. The global behavior of the system is illustrated by numerical simulations which confirm the local properties of the models near the equilibria.

Contents

1. Introduction

Chronologically, we can agree that the main predator-prey ecological models are those of Lotka-Volterra [26], Gause [7], Rozensweig-MacArthur [22] and finally the density-dependent model of Arditi-Ginzburg [1]. Andreï Kolmogorov [15] had focused his interest on very general systems modeling the different interactions of populations. A number of modifications have been made to these differential systems in order to theoretically answer new questions of a biological nature or to remove certain paradoxes inherent in these models. Among them, the case of a non-constant mortality rate of the predator. In this article, we consider the generalized Gause

Date: September 29, 2022.

2020 *Mathematics Subject Classification.* 34C05, 34D20, 34C23, 92D25.

Key words and phrases. predator-prey models, Rosenzweig-MacArthur stability criterion, general variable mortality rate, Poincaré-Andronov-Hopf bifurcation.

Model [7] :

$$\begin{cases} \dot{x} = g(x) - yp(x), \\ \dot{y} = [q(x) - m]\, y, \end{cases} \tag{1}$$

where the variables x and y are the density of prey and predator species respectively. The function g is the growth rate of the prey population, the function p is the functional response of the predator and the function q is the rate of conversion of prey to predator or the growth rate of the predator. The function g is of logistic type and the functions p and q are increasing and vanish at 0. The dot represents the derivative with respect to time: $\dot{x} = dx/dt$, and $\dot{y} = dy/dt$. For the background on this model, see [7]. For the case where the function p is not smooth in 0, which presents interesting behaviors because of the non-uniqueness of the solutions along the axis $x = 0$, the reader is referred to [4].

We extend (1) by replacing the constant mortality rate m by a disappearance or mortality rate $d(x, y)$ that may vary according to the density of the species. The term $d(x, y)$ can have different interpretations according to the models, as the intraspecific competition for resources and territory. It is legitimate to assume that the predator mortality rate is non-negative, decreasing with increasing prey density and increasing with increasing predator density, which will be specified in the assumptions on $d(x, y)$. We propose in Table 1 different expressions of d found in the literature. Explanations and comments on the models presented in this table are given in the appendix.

For (1), the well-known Rosenzweig-MacArthur graphical criterion asserts that a positive equilibrium point is locally exponentially stable if and only if it is located on a descending branch of the prey isocline, see [7], Section 4.4. For the more general case with a nonconstant mortality rate we bring out arcs of the ascending branches of the prey isocline outside of which a positive equilibrium is locally exponentially stable, provided that the slope of the prey isocline at that point is smaller than that of the predator isocline. Hence, a positive equilibrium could be attractive even if it is located on an ascending branch of the prey isocline.

The paper is organized as follows. In Section 2 we present the Rosenzweig-MacArthur graphical criterion of stability of a positive hyperbolic equilibrium. In Section 3, we examine the occurrence of a Poincaré-Andronov-Hopf bifurcation for the general model and compute the first Lyapunov coefficient ρ. If $\rho \neq 0$, the system undergoes a non degenerate Poincaré-Andronov-Hopf bifurcation at a certain positive equilibrium point. In Section 4, we illustrate the applicability of the previous results obtained for the general model to different particular models with the disappearance rates given in Table 1 : we use our graphical criterion to compare the local stability results with those of the examples and, for some of these models, we also compare the first Lyapunov coefficients. The global behavior is illustrated by numerical simulations that confirm the local properties of the models near the equilibria.

2. Model and main properties

We consider the generalized Gause model (1) in which we take into account a variable disappearance rate $d(x, y)$ in the predator equation. The model is therefore as follows :

$$\begin{cases} \dot{x} = g(x) - yp(x), \\ \dot{y} = [q(x) - d(x, y)]\, y. \end{cases} \tag{2}$$

The model (2) satisfies the following assumptions :

- H_1 : g is a C^1 function such that $g(0) = 0$, $g'(0) > 0$, and there exists $K > 0$ such that $g(K) = 0$ and $(x - K)g(x) < 0$ if $x \neq K$ with $g'(K) < 0$.
- H_2 : p and q are C^1 functions such that $p(0) = q(0) = 0$, $p'(x) > 0$ and $q'(x) > 0$ for all $x \geq 0$.
- H_3 : d is a positive C^1 function such that for all $(x, y) \in \mathbb{R}_+ \times \mathbb{R}_+$, $d(0, 0) > 0$, $d_x(x, y) := \frac{\partial d}{\partial x}(x, y) \leq 0$ and $d_y(x, y) := \frac{\partial d}{\partial y}(x, y) \geq 0$.

The assumption H_1 means that the growth function g is of logistical type. As a consequence of H_2, we have

$$\lim_{x\to+\infty} q(x) = q_\infty, \qquad 0 < q_\infty \leq +\infty, \tag{3}$$

and the function q admits an inverse function

$$q^{-1} : [0, q_\infty) \to \mathbb{R}^+, \qquad q^{-1}(0) = 0, \qquad (q^{-1})' > 0.$$

The inequality $d_x(x, y) \leq 0$ means that the mortality rate decreases when the density of prey increases for a fixed number of predators. The inequality $d_y(x, y) \geq 0$ means that the mortality rate increases when the density of predators increases for a fixed number of prey. Finally, the smoothness of g, p, q and d insures uniqueness property of the solutions of (2).

2.1. **Positivity and boundedness.** The first theorem deals with the positiveness and the boundedness of the solutions of (2).

Proposition 1. *Under the assumptions $H_1 - H_3$, the solutions of (2) are non-negative and asymptotically bounded.*

Proof. The axes $x = 0$ and $y = 0$ being invariant for the model (2), the positive cone is invariant. According to H_1, the growth function is of logistical type and using H_2 and the comparison lemma, we can prove that

$$\limsup_{t\to+\infty} x(t) \leq K, \tag{4}$$

that is the component $x(t)$ is asymptotically bounded above. To show that $y(t)$ is asymptotically bounded one can use a phase plane analysis similar to that given in [7], pp. 78-80. □

2.2. **Existence and stability of equilibria.** In the following, we give conditions for the existence and stability of the boundary and positive equilibrium points. The equilibria of (2) are the intersection points of the isoclines $\dot{x} = 0$ and $\dot{y} = 0$. The isocline $\dot{x} = 0$ is the union of the semi-axis $x = 0$ and the curve $y = h(x)$ where

$$h(x) := \frac{g(x)}{p(x)} \ \textit{if}\ x \neq 0, \quad h(0) = \frac{g'(0)}{p'(0)} > 0. \tag{5}$$

The isocline $\dot{y} = 0$ is the union of the semi-axis $y = 0$ and the curve of equation $U(x, y) = 0$, where U is defined by

$$U(x, y) := q(x) - d(x, y). \tag{6}$$

As a consequence of H_3, the limit

$$m := \lim_{x\to+\infty} d(x, 0) \geq 0$$

exists. Assume that $m < q_\infty$, where q_∞ is defined by (3). Hence, $x \mapsto d(x, 0)$ is decreasing from $d(0, 0) > 0$ to $m \in [0, q_\infty)$. Since q is strictly increasing from 0 to q_∞, equation $q(x) = d(x, 0)$ admits a unique solution which is denoted x_1:

$$x = x_1 \Longleftrightarrow q(x) = d(x, 0). \tag{7}$$

Let us prove that under assumptions H_2 and H_3, the equation $U(x, y) = 0$ defines a function $x = \varphi(y)$, such that $x_1 = \varphi(0)$. More precisely, we have the following result.

Lemma 1. *Assume that $m < q_\infty$. There exists a C^1 function*

$$\varphi : [0, y_\infty) \to \mathbb{R}+, \qquad 0 < y_\infty \leq +\infty, \qquad \varphi(0) = x_1, \tag{8}$$

such that, for all $y \in [0, y_\infty)$, we have $U(\varphi(y), y) = 0$, where U is defined by (6), and

$$\varphi'(y) = \frac{d_y(\varphi(y), y)}{[q'(\varphi(y)) - d_x(\varphi(y), y)]}. \tag{9}$$

Proof. Consider the set

$$I = \{y : \lim_{x\to+\infty} d(x,y) < q_\infty\},$$

where q_∞ is defined by (3). This set is not empty since $0 \in I$. Consider $y_\infty = \sup I$. For any $y \in [0, y_\infty)$, we have

$$d(\infty, y) := \lim_{x\to+\infty} d(x,y) < q_\infty.$$

Therefore, the function $x \mapsto d(x,y)$ is decreasing from $d(0,y) > 0$ to $d(\infty,y) < q_\infty$. Since q is strictly increasing from $q(0) = 0$ to q_∞, for any $y \in [0, y_\infty)$, the equation $q(x) = d(x,y)$ admits a unique solution, denoted $x = \varphi(y)$. Using the Implicit Function Theorem, we prove that the function $y \mapsto \varphi(y)$ is C^1 and that its derivative is given by (9). □

Remark 1. The isocline $U(x,y) = 0$ is the curve of equation $x = \varphi(y)$. If d does not depend on x the function φ is simply given by

$$\varphi(y) = q^{-1}(d(y)). \tag{10}$$

Moreover, if $d_y(x,y) > 0$, then the isocline $x = \varphi(y)$ can be also seen as a curve of equation $y = \psi(x)$. The function ψ is simply the inverse of the function φ and we have $\psi'(x) = 1/\varphi'(y)$. See Table 1 for the expressions of φ and ψ for various examples of the function d, that were considered in the literature.

Theorem 1. *Under the assumptions H_1 to H_3, the model (2) has the equilibria $E_1(0,0)$, $E_2(K,0)$ that always exist. A positive equilibrium exists if and only if*

$$x_1 < K, \tag{11}$$

where x_1 is defined by (7). Let $E^*(x^*,y^*)$ be a positive equilibrium. Then, $x^* \in [x_1, K)$ is a solution of equation $x = \varphi(h(x))$ and $y^* = h(x^*)$.

Proof. By H_1, the boundary equilibria are $E_1(0,0)$ and $E_2(K,0)$. According to H_2, H_3 and (9), $\varphi'(y) \geq 0$. Hence, $\varphi(y)$ is non-decreasing. A necessary and sufficient condition to have at least one non trivial intersection of the isoclines $y = h(x)$ and $x = \varphi(y)$ is that $x_1 < K$. Hence, under the condition (11), there exists at least a positive equilibrium point designated by $E^*(x^*,y^*)$. Thus, $x^* = \varphi(y^*)$ and $y^* = h(x^*)$. Therefore, $x^* \in [x_1, K)$ and $x^* = \varphi(h(x^*))$. □

The graphics in Fig. 1 represent some typical situations showing the isoclines $\dot{x} = 0$ (in blue) and $\dot{y} = 0$ (in red). An equilibrium is at the intersection of a blue curve and a red curve. The

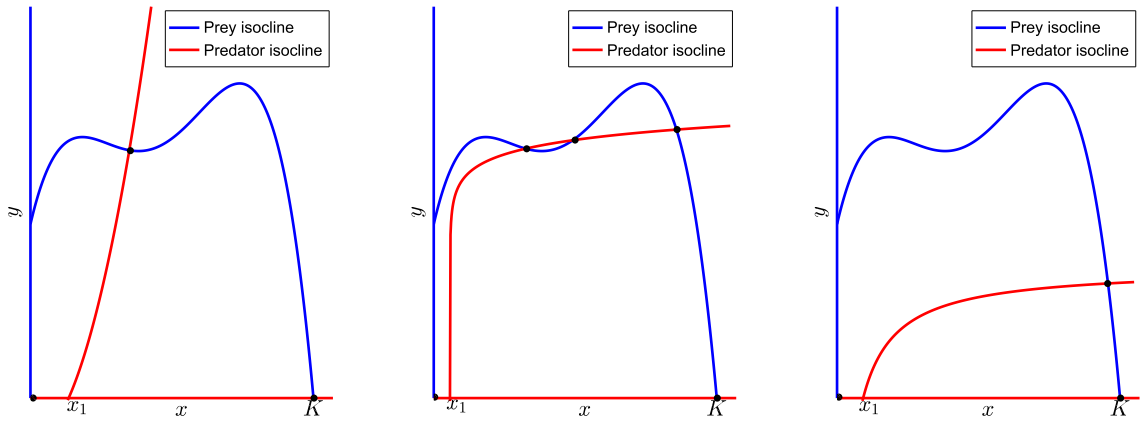

FIGURE 1. Schematic figures of isoclines of (2) and equilibria under condition (11).

following result gives the stability properties of the equilibria.

Theorem 2. *Under the assumptions H_1, H_2, H_3, the equilibrium E_1 is a saddle point of stable separatrix the y semi-axis and of unstable separatrix the open segment $(0, K)$ of the x-semi-axis. E_2 is locally exponentially stable (LES) if and only if $x_1 > K$ and it is a saddle point if $x_1 < K$, the stable separatrix of which is the x-semi-axis. If $x_1 < K$, E^* exists, it is LES if and only if*

$$\varphi'(y^*)h'(x^*) < 1, \tag{12}$$

and

$$\frac{p(x^*)h'(x^*)}{h(x^*)} < d_y(x^*, h(x^*)). \tag{13}$$

Proof. The Jacobian matrix of (2) at (x, y) is

$$\mathcal{J}(x,y) = \begin{pmatrix} p(x)h'(x) + p'(x)\,[h(x) - y] & -p(x) \\ [q'(x) - d_x(x,y)]\,y & q(x) - d(x,y) - d_y(x,y)y \end{pmatrix}. \tag{14}$$

First, using H_2 and H_3, the Jacobian matrix (14) at $E_0(0,0)$ is

$$\mathcal{J}(0,0) = \begin{pmatrix} h(0)p'(0) & 0 \\ 0 & -d(0,0) \end{pmatrix},$$

the eigenvalues of which are $\lambda_1 = h(0)p'(0)$ and $\lambda_2 = -d(0,0)$. From H_2 and (5) we have $\lambda_1 < 0$. From H_3 we have $\lambda_2 < 0$. Then, E_1 is a saddle point with separatrices indicated in the statement of the theorem. Similarly, using H_1 and H_3, the Jacobian matrix (14) at $E_2(K,0)$ is given by

$$\mathcal{J}(K,0) = \begin{pmatrix} p(K)h'(K) & -P(K) \\ 0 & q(K) - d(K,0) \end{pmatrix}, \tag{15}$$

the eigenvalues of which are $\lambda_1 = p(K)h'(K)$ and $\lambda_2 = q(K) - d(K,0)$. From H_2 and $h'(K) = g'(K)/p(K) < 0$, we have $\lambda_1 < 0$. Hence, E_2 is LES if and only if $\lambda_2 < 0$, i.e. $q(K) < d(K,0)$, which is equivalent to (11). If $x_1 < K$, then it is a saddle point with the x semi-axis as the stable separatrix. Let us now examine the stability of any positive equilibrium $E^*(x^*, y^*)$. The Jacobian matrix (14) at E^* can be written as

$$\mathcal{J}(x^*,y^*) = \begin{pmatrix} p(x^*)h'(x^*) & -p(x^*) \\ [q'(x^*) - d_x(x^*,y^*)]\,y^* & -d_y(x^*,y^*)y^* \end{pmatrix},$$

with $y^* = h(x^*)$. The determinant and trace of this matrix are given by

$$\det \mathcal{J}(x^*,y^*) = h\,(x^*)\,p(x^*)\left[q'(x^*) - d_x\,(x^*, h\,(x^*)) - h'\,(x^*)\,d_y\,(x^*, h\,(x^*))\right], \tag{16}$$

$$\operatorname{tr} \mathcal{J}(x^*,y^*) = p(x^*)h'(x^*) - h(x^*)d_y(x^*, h(x^*)). \tag{17}$$

Since $h\,(x^*)\,p(x^*) > 0$, we have

$$\det \mathcal{J}(x^*,y^*) > 0 \Longleftrightarrow h'(x^*)d_y(x^*,y^*) < q'(x^*) - d_x(x^*,y^*).$$

Dividing by $q'(x^*) - d_x(x^*,y^*)$ which is positive, according to H_2 and H_3, we obtain

$$\det \mathcal{J}(x^*,y^*) > 0 \Longleftrightarrow \frac{d_y(x^*,y^*)}{q'(x^*) - d_x(x^*,y^*)}h'(x^*) < 1.$$

Using (9) and $x^* = \varphi(y^*)$, we obtain the condition (12). We also have

$$\operatorname{tr} \mathcal{J}(x^*,y^*) < 0 \Longleftrightarrow p(x^*)h'(x^*) < h(x^*)d_y(x^*, h(x^*)).$$

Dividing by $h(x^*)$ which is positive, we obtain the condition (13) of the theorem. □

Remark 2. In the Rosenzweig-MacArthur case (RMA) (i.e. $d(x,y) = m$), we have $\varphi'(y) = 0$, so that condition (12), which is equivalent to $\det \mathcal{J}(x^*,y^*) > 0$, is always verified. Moreover, condition (13), which is equivalent to $\operatorname{tr} \mathcal{J}(x^*,y^*) < 0$, is equivalent to $h'(x^*) < 0$. Thus, E^* is LES if and only if it belongs to a decreasing branch of the isocline of the prey. This condition is known in the literature as the Rosenzweig-MacArthur graphical criterion, see Section 4.4 in [7].

We have the following result.

Proposition 2. *If the positive equilibrium point of (2) is located on a descending branch of the isocline of the prey isocline then it is LES.*

Proof. From H_2 and H_3, we have $p(x^*) > 0$, $\varphi'(x^*) > 0$ and $d_y(x^*, h(x^*)) \geq 0$. Therefore, if $h'(x^*) < 0$, then conditions (12) and (13) are satisfied. From Theorem 2 we deduce that E^* is LES. □

When d is not constant, conditions $\det \mathcal{J}(x^*, y^*) > 0$ and $\operatorname{tr} \mathcal{J}(x^*, y^*) < 0$ can also be satisfied when $h'(x^*) > 0$. We deduce that E^* can be LES, even if it belongs to an ascending branch of the isocline of the prey. Our aim now is to give a graphical description of the conditions of stability of a positive equilibrium. Our conditions are extensions of the Rosenzweig-MacArthur graphical condition of stability of E^*. We begin by the graphical description of the condition on the determinant.

Proposition 3. *Let $T_1 = (1, h'(x^*))$ and $T_2 = (\varphi'(y^*), 1)$ be the director vectors of the tangents of the prey and predator isoclines at $E^*(x^*, y^*)$, respectively. Condition (12) is equivalent to condition $\det(T_1, T_2) > 0$, i.e. (T_1, T_2) is a basis with the same orientation as the canonical basis. If, in addition $d_y(x^*, y^*) > 0$, then condition (12) is equivalent to condition $\psi'(x^*) > h'(x^*)$, where $y = \psi(x)$ is the equation of the predator isocline.*

Proof. We have $\det(T_1, T_2) = 1 - \varphi'(y^*)h'(x^*)$. Therefore (12) is equivalent to condition $\det(T_1, T_2) > 0$. If, in addition, $d_y(x^*, y^*) > 0$, then in a neighborhood of (x^*, y^*) the function φ has an inverse function ψ and $\psi'(x^*) = 1/\varphi'(y^*)$. Therefore, the condition $\varphi'(y^*)h'(x^*) < 1$ is equivalent to the condition $\psi'(x^*) > h'(x^*)$. □

Proposition 3 means that the determinant is positive if and only if, at the equilibrium point, the slope of the prey isocline is smaller than that of the predator isocline. Now we give the graphical description of the condition on the trace. We need the following definitions: the functions $H, G : [0, K) \to \mathbb{R}$ are given by

$$H(x) = \frac{p(x)h'(x)}{h(x)}, \quad G(x) = d_y(x, h(x)). \tag{18}$$

Proposition 4. *Let $\mathcal{A}$ be the closed subset of the prey isocline defined by*

$$\mathcal{A} = \{(x, h(x)) : x \in [0, K) \text{ and } H(x) \geq G(x)\}. \tag{19}$$

Condition (13) *is satisfied if and only if $E^* \notin \mathcal{A}$.*

Proof. Using the definitions (18) of the functions H and G, the condition (13) can be written $H(x^*) < G(x^*)$, which is equivalent to $E^* \notin \mathcal{A}$. □

Notice that $\mathcal{A}$ is necessarily a subset of the ascending part of the prey isocline. Proposition 4, asserts that the trace is positive if and only if the equilibrium point belongs to the interior of the set $\mathcal{A}$. The combination of Propositions 3 and 4 gives a geometric criterion of stability of a positive hyperbolic equilibrium point. It is an extension of the Rosenzweig-MacArthur graphical condition of stability to predator and prey models with a non constant mortality rate of the predator.

Theorem 3. *Let E^* be any positive equilibrium of* (2).

- *If, at E^*, the slope of the prey isocline is larger than that of the predator isocline, then E^* is a saddle point.*
- *If, at E^*, the slope of the prey isocline is smaller than that of the predator isocline and $E^* \notin \mathcal{A}$, then E^* is LES (a stable focus or node).*
- *If, at E^*, the slope of the prey isocline is smaller than that of the predator isocline and $E^* \in int\mathcal{A}$, then E^* is a repeller (an unstable focus or node).*

Proof. If the slope of the prey isocline is larger than that of the predator isocline, then, using Proposition 3, the determinant is negative, so that E^* is a saddle point. If the slope of the prey isocline is smaller than that of the predator isocline, then, using Proposition 3, the determinant is positive and two sub-cases must be distinguished. If $E^* \in int\mathcal{A}$, then, using Proposition 4, the trace is negative, so that E^* is LES. On the other hand, if E^* is in the interior of $\mathcal{A}$, then, using Proposition 4, the trace is positive, so that E^* is a repeller. □

Remark 3. If at a positive equilibrium point the isoclines of the prey and predator are tangent, the determinant is zero. This point corresponds to saddle node bifurcations. If a positive equilibrium belongs to the boundary of $\mathcal{A}$, the trace is zero. If, in addition, at this equilibrium point, the slope of the prey isocline is smaller than that of the predator isocline, then this point corresponds to the possibility of a Poincaré-Andronov-Hopf bifurcation.

3. Poincaré-Andronov-Hopf bifurcation (PAH)

In this section, we want to take a close look at the possibility of having a PAH bifurcation of the general model (2) under some additional hypotheses. Recall that, this bifurcation is characterized by an appearance or disappearance of a limit cycle from an equilibrium, changing its stability via a pair of purely imaginary eigenvalues. Hence, we assume that there exists a positive equilibrium $\tilde{E} = (\tilde{x}, \tilde{y})$ at which the following properties are satisfied

$$\det \mathcal{J}(\tilde{x}, \tilde{y}) > 0 \quad \text{and} \quad \operatorname{tr} \mathcal{J}(\tilde{x}, \tilde{y}) = 0. \tag{20}$$

Recall that $x = \tilde{x} \in [x_1, K)$ is a solution of equation $\varphi(h(x)) = x$, and $\tilde{y} = h(\tilde{x})$. We use the following notations.

$$\begin{array}{l} p_0 = p(\tilde{x}), \quad p_1 = p'(\tilde{x}), \quad p_2 = p''(\tilde{x}), \\ q_0 = q(\tilde{x}), \quad q_1 = q'(\tilde{x}), \quad q_2 = q''(\tilde{x}), \\ h_0 = h(\tilde{x}), \quad h_1 = h'(\tilde{x}), \quad h_2 = h''(\tilde{x}), \quad h_3 = h'''(\tilde{x}), \\ d_1 = d_x(\tilde{x}, \tilde{y}), \quad d_2 = d_y(\tilde{x}, \tilde{y}), \\ d_{11} = d_{xx}(\tilde{x}, \tilde{y}), \quad d_{12} = d_{xy}(\tilde{x}, \tilde{y}), \quad d_{22} = d_{yy}(\tilde{x}, \tilde{y}), \\ d_{112} = d_{xxy}(\tilde{x}, \tilde{y}), \quad d_{122} = d_{xyy}(\tilde{x}, \tilde{y}), \quad d_{222} = d_{yyy}(\tilde{x}, \tilde{y}). \end{array} \tag{21}$$

With these notations the determinant of the Jacobian matrix $\mathcal{J}(\tilde{x}, \tilde{y})$, denoted as ω^2, since it is positive, can be written as follows, see (16):

$$\omega^2 = \det \mathcal{J}(\tilde{x}, \tilde{y}) = p_0 h_0 (q_1 - d_1 - h_1 d_2) > 0. \tag{22}$$

We define now the first Lyapunov coefficient ρ given by

$$\rho = \frac{1}{16 p_0 \omega^2} \left(p_0 h_0 b_0 + h_0 b_1 d_2 + h_0^2 b_2 d_2^2 + (2 h_0 d_{122} - p_2)\, h_0^3 d_2^3 \right), \tag{23}$$

where the coefficients b_0, b_1 and b_2, are given by

$$\begin{aligned} b_0 &= 2p_0 p_1 q_1 h_2 + p_0^2 q_1 h_3 - p_0^2 q_2 h_2 + \left(p_0^2 h_2 - p_0 h_0 d_{12}\right) d_{11} \\ &\quad + (p_0 q_2 - q_1 h_0 d_{22})\, h_0 d_{12} - 2 q_1^2 h_0 d_{22} - p_0 q_1 h_0 d_{112} - q_1^2 h_0^2 d_{222} \\ &\quad - \left(p_0^2 h_3 + 2 p_0 p_1 h_2 - p_0 h_0 d_{112} - h_0^2 d_{12} d_{22} - 2 q_1 h_0^2 d_{222} - 4 q_1 h_0 d_{22}\right) d_1 \\ &\quad - (h_0 d_{222} + 2 d_{22})\, h_0 d_1^2, \\ b_1 &= p_0 p_2 q_1 h_0 + p_0^3 h_2^2 - p_0 p_1 q_2 h_0 - p_0^2 q_1 h_2 + p_0 p_1 h_0 d_{11} + p_0 h_0 (p_0 h_2 - 2 q_1) d_{12} \\ &\quad + (p_1 q_1 + p_0 q_2) h_0^2 d_{22} - 2 p_0 h_0^2 d_{12}^2 - q_1 h_0^3 d_{22}^2 - p_0 h_0^2 d_{11} d_{22} - 2 p_0 q_1 h_0^2 d_{122} \\ &\quad + \left(p_0^2 h_2 - p_0 p_2 h_0 - p_1 h_0^2 d_{22} + h_0^3 d_{22}^2 + 2 p_0 h_0 d_{12} + 2 p_0 h_0^2 d_{122}\right) d_1, \\ b_2 &= p_0 q_2 - p_0 p_1 h_2 - p_0^2 h_3 - p_0 d_{11} + 2 p_1 h_0 d_{12} + q_1 h_0 d_{22} - 2 h_0^2 d_{12} d_{22} \\ &\quad + q_1 h_0^2 d_{222} + p_0 h_0 d_{112} - (d_{22} + h_0 d_{222}) h_0 d_1. \end{aligned}$$

Note that ρ appears as a polynomial in d_2 of degree 3, whose coefficients are depending only on the other derivatives of d.

The occurrence of a PAH bifurcation is stated in the following proposition, where we simply choose x^* as a parameter bifurcation, where $E^*(x^*, y^*)$, with $y^* = h(x^*)$, is a positive equilibrium.

Theorem 4. *Let f, g and d be C^3, suppose that assumptions H_1-H_3 are satisfied and condition (11) holds, so that the system has at least one positive equilibrium, denoted $\tilde{E}(\tilde{x}, \tilde{y})$, with $\tilde{y} = h(\tilde{x})$*

and $\tilde{x} \in [x_1, K)$. *Suppose that* $\tilde{x}$ *satisfies the following conditions*

$$\det \mathcal{J}(\tilde{x}, \tilde{y}) > 0 \Longleftrightarrow q'(\tilde{x}) - d_x(\tilde{x}, \tilde{y}) - h'(\tilde{x}) d_y(\tilde{x}, \tilde{y}) > 0, \tag{24}$$

$$\operatorname{tr} \mathcal{J}(\tilde{x}, \tilde{y}) = 0 \Longleftrightarrow H(\tilde{x}) = G(\tilde{x}), \tag{25}$$

and the transversality condition

$$H'(\tilde{x}) \neq G'(\tilde{x}), \tag{26}$$

where H *and* G *are defined by (18). Then, the model (2) undergoes a PAH bifurcation when* x^* *crosses the value* $\tilde{x}$. *Moreover, if the parameter* ρ, *defined by* (23) *is non-zero, then the bifurcation is non degenerate: if* $\rho < 0$, *then the bifurcation is supercritical, while if* $\rho > 0$, *it is subcritical.*

Proof. The proof is given in Appendix A □

As a consequence of Theorem 4, we obtain the existence of limit cycles for (2). More precisely, we can make the following remark.

Remark 4. If $H'(\tilde{x}) > G'(\tilde{x})$, then

- if $\rho < 0$, then there exists $\tilde{x}_1 > \tilde{x}$ such that if $x^* \in (\tilde{x}, \tilde{x}_1)$ then the corresponding equilibrium $E^*(x^*, h(x^*))$ is unstable and is surrounded by a stable limit cycle,
- while if $\rho > 0$, then there exists $\tilde{x}_1 < \tilde{x}$ such that if $x^* \in (\tilde{x}_1, \tilde{x})$ then the corresponding equilibrium $E^*(x^*, h(x^*))$ is stable and is surrounded by a repelling limit cycle.

Similarly if $H'(\tilde{x}) < G'(\tilde{x})$, then

- if $\rho < 0$, then there exists $\tilde{x}_1 < \tilde{x}$ such that if $x^* \in (\tilde{x}_1, \tilde{x})$ then the corresponding equilibrium $E^*(x^*, h(x^*))$ is unstable and is surrounded by a stable limit cycle,
- while if $\rho > 0$, then there exists $\tilde{x}_1 > \tilde{x}$ such that if $x^* \in (\tilde{x}, \tilde{x}_1)$ then the corresponding equilibrium $E^*(x^*, h(x^*))$ is stable and is surrounded by a repelling limit cycle.

4. Some specific examples

In this section, we illustrate the applicability of our results obtained for the previous general model to different particular models with the disappearance rates given in Table 1. This table also gives the equation $x = \varphi(y)$ of the predator isocline and also its equation $y = \psi(x)$, if it exists.

Table 1. Different disappearance rates existing in the literature and the corresponding predator isocline.

Model	$d(x, y)$	$x = \varphi(y)$	$y = \psi(x)$
Gause or RMA [7, 16, 18, 22, 23, 28]	m	$x = q^{-1}(m)$	Does not exist
Hsu [11]	$d(x)$	$x = x_1$, see (7)	Does not exist
Bazykin [2, 3, 9, 19, 27]	$m + \alpha y$	$x = q^{-1}(m + \alpha y)$	$y = \frac{q(x) - m}{\alpha}$
Cavani Farkas [5, 6]	$m + \frac{\alpha y}{1+y}$	$x = q^{-1}\left(m + \frac{\alpha y}{1+y}\right)$	$y = \frac{q(x) - m}{\alpha + m - q(x)}$
Variable Territory [13, 24, 25]	$m + \frac{\alpha y}{\delta + x}$	Exists, see Lemma 1	$y = \frac{(q(x) - m)(\delta + x)}{\alpha}$

To illustrate our results we will consider the case where the growth function g is given by the logistic growth function, the functional response p is given by the Holling II functional response and the growth function of the predator q is proportional to p. More precisely

$$g(x) = rx\left(1 - \tfrac{x}{K}\right), \qquad p(x) = \tfrac{ax}{c+x}, \qquad q(x) = ep(x) = \tfrac{eax}{c+x}, \tag{27}$$

where the parameters r, K, a, c and e are all positive biological parameters. More exactly, r is the growth rate per capita of the prey, K is the carrying capacity of the prey, a is the maximum rate of prey consumption per unit of predator biomass, c is the half saturation constant for the prey and e is the rate of conversion of prey to predator. Assumptions H_1 and H_2 are clearly satisfied by functions (27). One can easily check that for all mortality rates $d(x, y)$ summarized in Table 1, the assumption H_3 is satisfied. From a biological point of view, it is interesting to consult the references indicated in Table 1 to know about the motivation of these models. Brief information is provided in Appendix B.

For the functions g and p given in (27), the prey isocline is the parabola $y = h(x)$ where h, defined by (5), becomes

$$h(x) = \tfrac{r}{aK}(K - x)(c + x). \tag{28}$$

The top of the parabola is obtained for $x = \hat{x}$, where $\hat{x}$, the solution of $h'(x) = 0$, is given by

$$\hat{x} := \tfrac{K-c}{2}. \tag{29}$$

For the function q given in (27), a positive equilibrium exists if the condition (11) of Theorem 1 is satisfied, that is

$$x_1 := q^{-1}(m) = \tfrac{mc}{ea-m} < K \iff \tfrac{eaK}{c+K} > m. \tag{30}$$

If $E^*(x^*, y^*)$ is a positive equilibrium, then $x_1 \leq x^* < K$, where x_1 is given in (30). The positive equilibria are obtained as the intersection of the prey isocline $y = h(x)$, where h is defined by (28), and the predator isocline which depends on functions q and d, is given in Table 1. Note that the function $\psi = \varphi^{-1}$ exists for all the models in Table 1, except for the RMA and Hsu models. In the case where q is as in (27), we can also obtain an explicit formula for φ by solving in x the equation $\frac{eax}{c+x} = d(x, y) + m$.

For the functions p and g given by (27), the function H defined by (18), is written

$$H(x) = \frac{ax(K - c - 2x)}{(K - x)(c + x)^2}.$$

Recall that H is defined on $[0, K)$. Suppose that $\hat{x} > 0$, where $\hat{x}$ is given by (29). The function H is positive for $x \in (0, \hat{x})$ and negative for $x \in (\hat{x}, K)$ and satisfies $H(0) = 0$ and $H(\hat{x}) = 0$. It is increasing, then decreasing on the interval $[0, \hat{x}]$. Moreover, according to assumption H_3, the function G defined in (18) is non-negative.

Let us determine the subset $\mathcal{A}$ of the ascending part of the prey isocline, defined by (19), where the trace is non-negative. We must solve the equation $H(x) = G(x)$. Its appears that this equation can have no or two real roots x_L and x_R in $[0, \hat{x}]$ (see the upper part of Fig. 2).

If this equation does not admit a solution, it means graphically, according to the properties of H and G, that the graph of G is above the one of H for $x \in [0, K]$. Consequently, the trace is always negative. If it admits a solutions, the subset $\mathcal{A}$, is the closed arc

$$\mathcal{A} = \{(x, h(x)) : x_L \leq x \leq x_R\}$$

of the ascending branch of the prey isocline. This arc is plotted in red in the lower part of Fig. 2 for some specific examples, while the complementary arc is plotted in blue. If an equilibrium belongs to the red arc, then the trace is positive. If it belongs to the blue arc, then the trace is negative. In Gause/RMA model and in Hsu model, x_L and x_R coincide with 0 and $\hat{x}$ respectively and we find that condition (13) is verified if and only if $x^* > \hat{x}$, since $\mathcal{A}$ consists of the increasing branch of the isocline of the prey. In Bazykin, CF and VT models, when $\alpha \to 0$, then $x_L \to 0$ and $x_R \to \hat{x}$, and we find the result of RMA model.

In all figures of the following subsections, we depicted the non-trivial prey isocline $y = h(x)$ and the non-trivial predator isocline $y = \psi(x)$, respectively in blue and black, the functions g, p and q being defined by (27). In addition to the boundary equilibria which both are saddle-points, the intersection of the non-trivial isoclines define positive equilibria plotted in blue dots when they are LES and in red dots when they are unstable. The figures show also the closed arc $\mathcal{A}$ of the ascending branch of the prey isocline, in red, outside which the trace condition (13) holds. We examine the change of the phase portraits by increasing the value of m, which will be

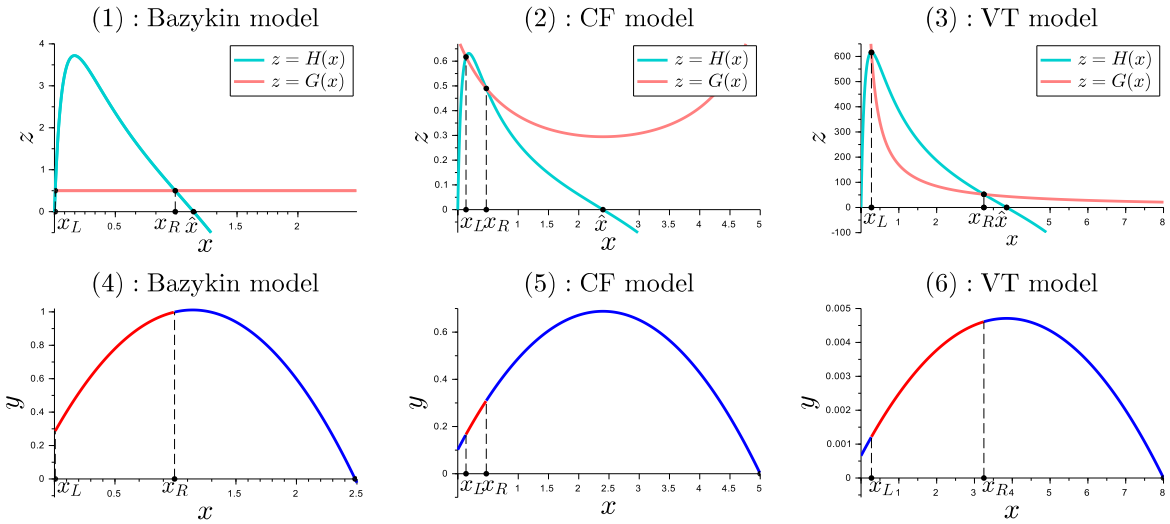

FIGURE 2. The graphs of the functions H and G for Bazykin, CF and VT models with the parameter values given in Table 2, 7, 10 and the corresponding arcs $\mathcal{A}$ on the prey isocline.

our bifurcation parameter. Note that, except for the example of Fig. 6 bellow, the ends points $(x_L, h(x_L))$ and $(x_R, h(x_R))$ of $\mathcal{A}$ do not change with m, since $H(x)$ and $G(x)$ do not.

4.1. **The Gause/RMA model.** In the Gause type model (1), $d(x, y) = m > 0$ does not depend on x and y. We have the following result.

Proposition 5. *For* (1)*, a PAH bifurcation can occur at* $\tilde{x}$*, if and only if* $h_1 := h'(\tilde{x}) = 0$*. We have*

$$\rho = \frac{1}{16}\left(2p_1h_2 + p_0h_3 - \frac{p_0q_2}{q_1}h_2\right). \tag{31}$$

Proof. For (1), we have $\det \mathcal{J}(\tilde{x}, \tilde{y}) > 0$ and $\operatorname{tr} \mathcal{J}(\tilde{x}, \tilde{y}) = 0$, if and only if $h'(\tilde{x}) = 0$. Moreover, we have $d_2 = 0$, so that only the first term $p_0h_0b_0$ in ρ, given by (23), must be considered. Using the fact that all derivatives of d are equal to 0, the coefficient b_0 is given by

$$b_0 = 2p_0p_1q_1h_2 + p_0^2q_1h_3 - p_0^2q_2h_2.$$

Now, using (22) we have $\omega^2 = p_0h_0q_1$. Therefore, using (23), we have

$$\rho = \frac{1}{16p_0^2h_0q_1}p_0h_0b_0 = \frac{1}{16p_0q_1}b_0,$$

which is the expression given in the proposition. □

The formula (31) for ρ, is known in the literature, see Equation (4.3) in [28]. If we replace in (31) p, q and h by their expressions given in (27) and (28) respectively, we obtain

$$\rho = -\frac{r}{2K(c+K)}.$$

Therefore, for the functions (27), the PAH bifurcation of (1) is always supercritical. However, for other growth functions it can be subcritical. It is the case, for example, for the trigonometric growth function $q(x) = a\tanh(bx)$, as shown in [23].

4.2. **The Hsu model.** In the Hsu model, i.e. $d(x, y) = d(x) > 0$ depends only on x and is decreasing, the system (2) is written

$$\begin{cases} \dot{x} = g(x) - yp(x), \\ \dot{y} = [q(x) - d(x)]\, y. \end{cases} \tag{32}$$

We have the following result.

Proposition 6. *For* (32)*, a PAH bifurcation can occur at* $\tilde{x}$*, if and only if* $h_1 := h'(\tilde{x}) = 0$*. We have*

$$\rho = \tfrac{1}{16(q_1-d_1)}\left(2p_1q_1h_2 + p_0q_1h_3 - p_0q_2h_2 - (p_0h_3 + 2p_1h_2)d_1 + p_0h_2d_{11}\right). \tag{33}$$

Proof. For (32), we have $\det \mathcal{J}(\tilde{x},\tilde{y}) > 0$ and $\operatorname{tr}\mathcal{J}(\tilde{x},\tilde{y}) = 0$, if and only if $h'(\tilde{x}) = 0$. Moreover, we have $d_2 = 0$, so that only the first term $p_0h_0b_0$ in ρ, given by (23), must be considered. Using the fact that all derivatives of d are equal to 0, except for d_1 and d_{11}, the coefficient b_0 is given by

$$b_0 = 2p_0p_1q_1h_2 + p_0^2q_1h_3 - p_0^2q_2h_2 - (p_0^2h_3 + 2p_0p_1h_2)d_1 + p_0^2h_2d_{11}.$$

Now, using (22) we have $\omega^2 = p_0h_0(q_1 - d_1)$. Therefore, using (23), we have

$$\rho = \frac{1}{16p_0^2h_0(q_1-d_1)}p_0h_0b_0 = \frac{1}{16p_0(q_1-d_1)}b_0,$$

which is the expression given in the proposition. □

To our knowledge, the formula (33) for ρ, is not known in the existing literature. If we replace in (33) p, q and h by their expressions given in (27) and (28) respectively, and $d(x)$ is given by

$$d(x) = m + \frac{\alpha}{\delta + x}, \tag{34}$$

we obtain

$$\rho = -\frac{r}{2K(c+K)}\frac{ace(c-K-2\delta)^3 + \alpha(c+K)\left[2c(c-K-2\delta) + (c+K)(c-K)\right]}{\left[ace(c-K-2\delta)^2 + \alpha(c+K)^2\right](c-K-2\delta)}.$$

ρ is then the product of two fractions, the first one $-r/\left[2K(c+K)\right]$ being negative. Moreover, knowing that $\hat{x}$ given by (29) is positive, one has $c - K < 0$, hence $c - k - 2\delta < 0$. This makes the numerator and the denominator of the second fraction clearly negative. Hence, ρ is always negative. Therefore, for the functions (27) and (34), the PAH bifurcation of (32) is always supercritical.

4.3. **The Bazykin model.** In this section we apply our findings to the Bazykin model [2, 3]. This model was studied in detail in [9] and in the the Kuznetsov book on bifurcation theory [17]. It has also been considered recently in [19, 27]. In these works, conditions for the existence and stability of equilibria are established, as a function of parameters, and bifurcation diagrams, with respect to one or two parameters, are constructed. Our aim is not to make a complete new study of the model, but to show how the graphical method we have developed allows us to clarify and complete certain results of the literature. In particular, when the parameters of the model are fixed, we construct the part of the ascending branch of the prey isocline, denoted $\mathcal{A}$ and shown in red in the figures, such that the trace of a positive coexistence equilibrium is positive, when this equilibrium is on this part. In the Bazykin model, i.e. $d(x,y) = m + \alpha y$, the system (2) is written

$$\begin{cases} \dot{x} = g(x) - yp(x), \\ \dot{y} = \left[q(x) - \alpha y - m\right] y. \end{cases} \tag{35}$$

We have the following result.

Proposition 7. *For* (35)*, a PAH bifurcation can occur at* $\tilde{x}$*, if and only if* $q_1 - \alpha h_1 > 0$ *and* $p_0h_1/h_0 = \alpha$*. We have*

$$\rho = \frac{1}{16(q_1 - \alpha h_1)}\left(c_0 + \frac{c_1}{p_0}\alpha + \frac{c_2}{p_0}\alpha^2 - \frac{p_2h_0^2}{p_0^2}\alpha^3\right), \tag{36}$$

where

$$\begin{aligned} c_0 &= 2p_1q_1h_2 + p_0q_1h_3 - p_0q_2h_2, \\ c_1 &= p_2q_1h_0 + p_0^2h_2^2 - p_1q_2h_0 - p_0q_1h_2, \\ c_2 &= q_2h0 - p_1h_0h_2 - p_0h_0h_3. \end{aligned}$$

Proof. For (35), we have

$$\det \mathcal{J}(\tilde{x},\tilde{y}) = p(\tilde{x})h(\tilde{x})\left[q'(\tilde{x}) - \alpha h'(\tilde{x})\right].$$

Therefore $\det \mathcal{J}(\tilde{x},\tilde{y}) > 0$ if and only if $q'(\tilde{x}) > \alpha h'(\tilde{x})$. On the other hand, we have

$$\operatorname{tr} \mathcal{J}(\tilde{x},\tilde{y}) = p(\tilde{x})h'(\tilde{x}) - \alpha h(\tilde{x}).$$

Therefore $\operatorname{tr} \mathcal{J}(\tilde{x},\tilde{y}) = 0$, if and only if $h'(\tilde{x}) = \alpha h(\tilde{x})/p(\tilde{x})$. Moreover, we have $d_2 = \alpha$. Using the fact that all other derivatives of d are equal to 0 we obtain

$$\begin{aligned} b_0 &= 2p_0p_1q_1h_2 + p_0^2q_1h_3 - p_0^2q_2h_2,\\ b_1 &= p_0p_2q_1h_0 + p_0^3h_2^2 - p_0p_1q_2h_0 - p_0^2q_1h_2,\\ b_2 &= p_0q_2 - p_0p_1h_2 - p_0^2h_3. \end{aligned}$$

Now, using (22) we have $\omega^2 = p_0h_0(q_1 - \alpha h_1)$. Therefore, using (23), we have

$$\rho = \frac{1}{16p_0^2(q_1 - \alpha h_1)}\left(p_0b_0 + b_1\alpha + h_0b_2\alpha^2 - p_2h_0^2\alpha^3\right),$$

which is the expression given in the proposition. □

To our knowledge, the formula (36) for ρ in the Bazykin case, is known in the literature only for the specific case where g, p and q are of the form (27), see [19]. In what follows we give more details and information on this issue and we show how our formula (36) reduces in this special case to the formula of [19]. The Bazykin model, with g, p and q given by (27), is written

$$\begin{aligned} \frac{dx}{dt} &= rx(1 - x/K) - \tfrac{ax}{c+x}y,\\ \frac{dy}{dt} &= \left(e\tfrac{ax}{c+x} - \alpha y - m\right)y. \end{aligned} \tag{37}$$

The difficulty in using formula (36) is that the value $\tilde{x}$ where the PAH bifurcation can occur is a solution of the equation $p_0h_1/h_0 = \alpha$, i.e. $H(x) = G(x)$, which is written

$$\frac{ax(K - c - 2x)}{(K - x)(c + x)^2} = \alpha. \tag{38}$$

This equation is equivalent to a third degree algebraic equation in x. To overcome this difficulty, and following [19], we parametrize the Bazykin model (37) as follows

$$\begin{aligned} \frac{dx}{dt} &= x(M - Nx) - \tfrac{B_1x}{Q+x}y,\\ \frac{dy}{dt} &= \left(\tfrac{B_2x}{Q+x} - \tfrac{1}{N}y - P\right)y, \end{aligned} \tag{39}$$

where

$$B_1 = (M - N)(Q + 1) \text{ and } B_2 = (P + 1/N)(Q + 1), \tag{40}$$

with $M > N > 0$, $P > 0$ and $Q > 0$, see the model (4.13) in [19]. There is a linear change of variable transforming system (37) in (39). The interest of the form (39) is that it has a positive equilibrium at $E(1, 1)$. The study of the PAH bifurcation around $(1, 1)$ in system (39), corresponds to the PAH bifurcation in (37) around a positive equilibrium where the determinant is positive and the trace is 0. This bifurcation occurs only if $H(1) = G(1) = 1/N$, which is equivalent to the following condition

$$M^* = \tfrac{N^2Q+2N^2+Q+1}{N}. \tag{41}$$

Now, we replace in (36), $\alpha = 1/N$, $\tilde{x} = 1$ and

$$g(x) = x(M - Nx), \quad p(x) = \frac{B_1x}{Q + x}, \quad q(x) = \frac{B_2x}{Q + x},$$

where B_1 and B_2 are defined by (40) and $M = M^*$, given by (41). We obtain the following expression for ρ,

$$\rho = -\frac{2(2N((N^2+1)Q^2+QN^2-N^2)+QP(1+N^2+2N^4+2N^2(N^2+1)Q))}{(Q+1)^2(Q+PNQ+QN^2+PN^3Q-1)},$$

which is the same, to a multiplicative positive factor, as the expression of the first Lyapunov coefficient σ_1 obtained by [19] in page 132.

Numerical simulations : In order to compare with some of the results in the literature, we choose the parameter values used in Figs. 4.5(a,d) of [19]. The parameters in (39), where B_1 and B_2 are given by (40), correspond to the following parameters in (37)

$$r = M, \quad K = \tfrac{M}{N}, \quad a = (M-N)(Q+1), \quad c = Q, \quad e = \tfrac{P+1/N}{M-N}, \quad \alpha = \tfrac{1}{N}, \tag{42}$$

and $m = P$. We use the values of M, N, P and Q, depicted in Table 2. These values are choosen such that Fig. 3(d), where $m = P = 0.25$, corresponds to Fig. 4.5(a) of [19] and Fig. 4(b), where $m = P = 4/3 - 0.07$, corresponds to Fig. 4.5(d) of [19].

TABLE 2. The values of the parameters r, K, a, c, e and α used in the Bazykin model (37) are given by (42), where M, N, P and Q are as in the table. The value of m is depicted on each figure.

Figure	M	N	P	Q
Figs. 2(1), 3	$5-0.03$	2	$1/4$	$1/5$
Figs. 4	$5-0.0015$	2	$4/3-0.07$	$1/5$

Recall that the abscissas x_L and x_R of the ends of the arc $\mathcal{A}$ are the roots of the third degree algebraic equation (38), which lay between 0 and $\hat{x}$, where $\hat{x}$ is given by (29).

We consider m as the bifurcation parameter. We give in Fig. 3 the plots corresponding to the values of the parameter r, K, a, c, e and α defined in Line 1 of Table 2 and various values of m, chosen such that the principal behaviors of the model are illustrated. For these parameter values, the abscissas x_L and x_R are given by $x_L = 0.0065$ and $x_R = 0.9924$, see Fig. 2(1) and 3. The corresponding bifurcation values m_L and m_R of m are obtained by solving equation $\psi(x_i) = h(x_i)$, $i = L, R$, with respect to m, where ψ is given in Table 1. For these parameter values, $m_L = -0.1151$ and $m_R = 0.2496$. The first value corresponds to the passage of the predator isocline through point $(x_L, h(x_L))$, that is to say for $\tilde{x} = x_L$. The second value corresponds to the passage of the predator isocline through point $(x_R, h(x_R))$, that is to say for $\tilde{x} = x_R$. Furthermore, the isocline of the predator is tangent to the isocline of the prey, which corresponds to a saddle-node bifurcation, when $m = 0.2468$ or $m = 0.2530$. These two values are obtained firstly by solving the equation $h'(x) = \psi'(x)$, with respect to x. This leads to solving a third degree algebraic equation. We keep only its positive roots noted by x_1^{SN} and x_2^{SN}. For these parameter values, $x_1^{SN} = 0.5149$ and $x_2^{SN} = 0.8534$. Then, by solving the equation $\psi(x_i^{SN}) = h(x_i^{SN})$, $i = 1, 2$, with respect to m, we obtain the two values of m stated above.

The results on the existence and stability of the positive equilibria are deduced from Theorem 3 and are summarized in Table 3.

Note that when $m < 0.2496$ the Poincaré-Bendixson theorem predicts that the system has at least one limit cycle that is stable in its exterior. Indeed, in this case the system has only unstable equilibria. Let us illustrate some of these behaviors by numerical simulations, which will also highlight homoclinic bifurcations.

For $m = 0.24$, the system has one positive equilibrium which is unstable, surrounded by a stable limit cycle (in blue). The unstable positive separatrix of $E_2(K, 0)$ (in green) converges towards this limit cycle, see Fig. 3(a).

For $m = 0.2474$, the system has three positive equilibria. The left and the right point are unstable, the middle one is a saddle. These equilibria are surrounded by the blue stable limit cycle, see Fig. 3(b and c). Note that the unstable positive separatrix of $E_2(K, 0)$ and the unstable separatrices (in magenta) of the interior saddle point converge towards the limit cycle, while the

TABLE 3. Positive equilibria and their stability of the Bazykin model for the parameter values given in Line 1 of Table 7.

m	Behavior of the system
$0 \leq m < 0.2468$	A unique positive (unstable) equilibrium
$m = 0.2468$	Saddle-node bifurcation
$0.2468 < m < 0.2496$	Three positive unstable equilibria
$m = 0.2496$	Subcritical PAH bifurcation ($\rho = 1.6678$)
$0.2496 < m < 0.2530$	Three positive equilibria, two unstable and one stable
$m = 0.2530$	Saddle-node bifurcation
$0.2530 < m$	A unique positive (stable) equilibrium

stable separatrices (in green) of the interior saddle point each converge towards one of the two unstable equilibria when $t \to -\infty$.

For $m = 0.25$, which corresponds to Fig. 4.5(a) in [19], the system has three positive equilibria. The left one is unstable, the middle one is a saddle point and the right one is LES. These equilibria are surrounded by a big stable limit cycle (in blue). The right equilibrium is surrounded by a small unstable limit cycle (in red) which has been created by a subcritical PAH bifurcation for $m = 0.2496$, see Fig. 3(d and g). Note that the unstable positive separatix of $E_2(K, 0)$ and the unstable separatrices of the interior saddle point converge towards the big limit cycle, while a stable separatrix of the interior saddle point converges towards the small cycle when $t \to -\infty$.

When the value of m increases, the unstable limit cycle grows and approaches to the unstable separatrix of the positive saddle point. When m crosses a value between 0.25167 and 0.25168, (see Fig. 3 (e and f) and their zooms), the unstable limit cycle disappears when meeting the saddle point by a homoclinic bifurcation.

For $m = 0.25167$, the stable separatrix is trapped between the unstable separatrix (magenta) and the small cycle.

For $m = 0.25168$, the unstable separatrix converges to the positive LES equilibrium and is surrounded by the stable separatrix. There has been a crossing of the separatrices, leading to the destruction of the unstable cycle. The stable big cycle also disappears through a homoclinic bifurcation which occurs for a value of m between 0.25214 and 0.25215, see Fig. 3 (j and l).

In Fig. 4, we consider the parameter values indicated in Line 2 of Table 2. For these parameter values, the abscissas of the ends of the arc $\mathcal{A}$, are given by $x_L = 0.0064$ and $x_R = 0.9996$. Note that the predator isocline passes through the ends of the arc $\mathcal{A}$ for $m = m_L = -0.0768$ or $m = m_R = 1.2632$. The first value corresponds to the passage of the predator isocline through point $(x_L, h(x_L))$, that is to say for $\tilde{x} = x_L$. The second value corresponds to the passage of the predator isocline through point $(x_R, h(x_R))$, that is to say for $\tilde{x} = x_R$. The results on the

TABLE 4. Positive equilibria and their stability of the Bazykin model for the parameter values given in Line 2 of Table 2.

m	Behavior of the system
$0 \leq m < 1.2632$	A unique positive (unstable) equilibrium
$m = 1.2632$	Subcritical PAH bifurcation ($\rho = 0.0213$)
$1.2632 < m$	A unique positive (stable) equilibrium

existence and stability of the positive equilibria are deduced from Theorem 3 and are summarized in Table 4.

When $m < 1.2632$, the Poincaré-Bendixson theorem predicts that the system has at least one limit cycle that is stable in its exterior and surrounding the unique unstable positive equilibrium. Numerical simulations in Fig. 4 illustrate these behaviours and also highlight a saddle node bifurcation of cycles.

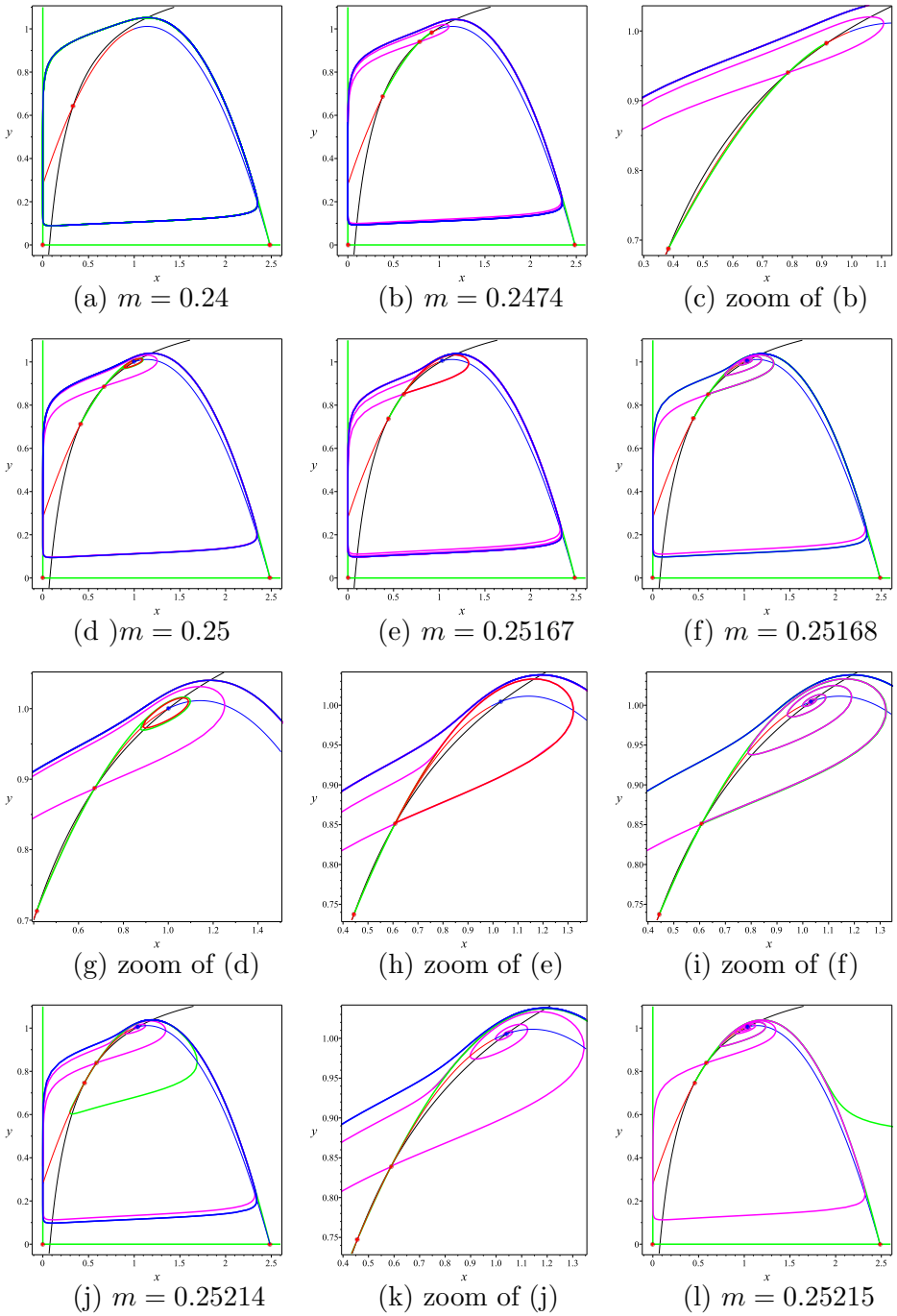

(a) $m = 0.24$ (b) $m = 0.2474$ (c) zoom of (b)

(d)$m = 0.25$ (e) $m = 0.25167$ (f) $m = 0.25168$

(g) zoom of (d) (h) zoom of (e) (i) zoom of (f)

(j) $m = 0.25214$ (k) zoom of (j) (l) $m = 0.25215$

FIGURE 3. Some phase portraits of Bazykin model with the parameter values given in Line 1 of Table 2.

For $m = 1.217$, the system has one positive equilibrium which is unstable and surrounded by a stable limit cycle (in blue). The unstable positive separatrix of $E_2(K, 0)$ (in green) converges towards this limit cycle, see Fig. 4(a).

For $m = 4/3 - 0.07$, which corresponds to Fig. 4.5(d) in [19], the system has one positive equilibrium which is LES and is surrounded by two limit cycles, a big stable one (in blue) and a small unstable one (in red). The small limit cycle has been created by a subcritical PAH bifurcation for $m = 1.2632$, see Fig. 4(b and c). Note that the unstable positive separatix of $E_2(K, 0)$ still converges towards the big limit cycle.

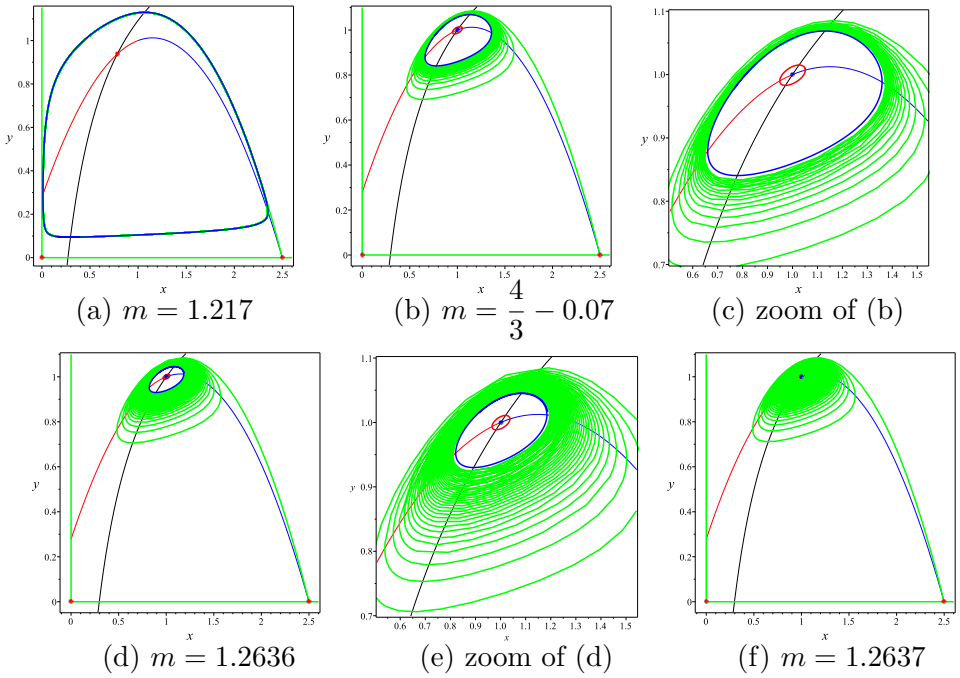

(a) $m = 1.217$ (b) $m = \frac{4}{3} - 0.07$ (c) zoom of (b)

(d) $m = 1.2636$ (e) zoom of (d) (f) $m = 1.2637$

FIGURE 4. Some phase portraits of Bazykin model with the parameter values given in Line 2 of Table 2.

For $m = 1.2636$, the cycles approach each other, the stable one getting smaller, and the unstable one getting bigger. The two cycles disappear through a saddle node bifurcation of cycles which occurs for a value of m between 1.2636 and 1.2637, see Fig. 4 (d, e and f).

For $m = 1.2637$, the unstable separatrix of $E_2(K, 0)$ converges to the positive LES equilibrium, see Fig. 4 (f).

The reader can find in [10] numerical illustrations for other sets of values of the numerical parameters of the Bazykin model.

4.4. **The Cavani-Farkas (CF) model.** In CF model, i.e. $d(x, y) = m + \frac{\alpha y}{1+y}$, the system (2) is written

$$\begin{cases} \dot{x} = g(x) - yp(x), \\ \dot{y} = \left[q(x) - \frac{\alpha y}{1+y} - m\right] y. \end{cases} \tag{43}$$

One could, as for the Bazykin model, write the particular form of the exponent ρ given by (23) in the case of (43) and g, p q given by (27). However, we do not do so, because the resulting expression is rather complicated. Furthermore, the equation $H(x) = G(x)$ defining the values x_L and x_R becomes now

$$\frac{ax(K - c - 2x)}{(K - x)(c + x)^2} = \frac{\alpha}{(1 + h(x))^2}, \tag{44}$$

where h is given by (28). It is a sixth degree algebraic equation in x. The values x_L and x_R are the roots that lay between 0 and $\hat{x}$, where $\hat{x}$ is given by (29) .

In Fig. 5, we give the principal behaviors of the model with the values of the parameters indicated in Line 1 of Table 7. These values were chosen to show the possibility of having homoclinic bifurcation in CF model. For these parameter values, the abscissas of the ends of the arc $\mathcal{A}$, are given by $x_L = 0.1365$ and $x_R = 0.4717$, see Fig. 2(2) and Fig. 5. Note that the predator isocline passes through the ends of the arc $\mathcal{A}$ if $m = m_L = 0.0473$ and $m = m_R = 0.0910$. The first value corresponds to the passage of the predator isocline through the point $(x_L, h(x_L))$, that is to say for $\tilde{x} = x_L$. The second value corresponds to the passage of the predator isocline through the point $(x_R, h(x_R))$. The bifurcation values m_L and m_R are

obtained by solving equation $\psi(x_i) = h(x_i)$, $i = L, R$, with respect to m. For the second value, $E^*(x_R, h(x_R))$ is a saddle point since $\det \mathcal{J}(x_R, h(x_R)) < 0$. Hence, the PAH bifurcation does not occur at $m = m_R$. Furthermore, the isocline of the predator is tangent to the isocline of the prey, which corresponds to a saddle-node bifurcation, when $m = 0.0368$ or $m = 0.0911$. These two values are obtained firstly by solving the equation $h'(x) = \psi'(x)$, with respect to m. We find a value of $m = m(x)$ that depends on x. Substituting $m(x)$ in ψ and solving the equation $h(x) = \psi(x)$ with respect to x, we only keep the positive roots, noted by x_1^{SN} and x_2^{SN}. With our parameter values, we find $x_1^{SN} = 2.1536$ and $x_2^{SN} = 0.4454$. Then, by solving the equation $\psi(x_i^{SN}) = h(x_i^{SN})$, $i = 1, 2$, with respect to m, we obtain the two values of m stated above.

TABLE 5. Positive equilibria and their stability of the CF model for the parameter values given in Line 1 of Table 7.

m	Behavior of the system
$0 < m < 0.0368$	A unique positive (stable) equilibrium
$m = 0.0368$	Saddle-node bifurcation
$0.0368 < m < 0.0473$	Three positive equilibria, two stable and one unstable
$m = 0.0473$	Supercritical PAH bifurcation ($\rho = -0.0272$)
$0.0473 < m < 0.0911$	Three positive equilibria, two unstable and one stable
$m = 0.0911$	Saddle-node bifurcation
$0.0911 < m$	A unique positive (stable) equilibrium

The results on the existence and stability of the positive equilibria are deduced from Theorem 3 and are summarized in Table 5. Here is an illustration of some of these behaviors by numerical simulations, which will also highlight homoclinic bifurcation.

For $m = 0.02$, the system has one positive equilibrium, which is LES and the unstable positive separatrix of $E_2(K, 0)$ (in green) converges towards this equilibrium, see Fig. 5, (a).

For $m = 0.038$, the system has three positive equilibria. The left and the right point are LES, the middle is a saddle, see Fig. 5, (b). Note that the unstable positive separatrix of $E_2(K, 0)$ converges towards the right LES point. The unstable separatrices (in magenta) each converges to one of the two LES equilibria.

For $m = 0.062$, the system has three positive equilibria. The left one is unstable, the middle one is a saddle point and the right one is LES. The left equilibrium is surrounded by a stable limit cycle (in blue) which has been created by a supercritical PAH bifurcation for $m = 0.0473$, see Fig. 5, (c). The unstable positive separatrix of $E_2(K, 0)$ converges towards the right equilibrium while the unstable separatrices converge one towards the limit cycle, the other towards the LES equilibrium. When the value of m increases, the stable limit cycle grows and approaches the unstable separatrix of the positive saddle point.

When m crosses a value between 0.066 and 0.067, (see Fig. 5, (d and f) and their zooms), the stable limit cycle disappears when meeting the saddle point by a homoclinic bifurcation. There has been a crossing of the stable and unstable separatrices.

For $m = 0.12$, the system has one positive equilibrium which is LES, the unstable positive separatrix of $E_2(K, 0)$ converges towards this equilibrium, see Fig. 5, (h).

Actually, for the CF model, as written for example in [6], $\alpha = \delta - m$, where δ is a constant, and thus depends on m. It is the case of the parameter values indicated in Line 2 of Table 7, for which the bifurcation diagram of Fig. 3 (a) was dressed in [6]. The authors gave there the bifurcation values $m_1 = 0.5806$ and $m_2 = 2.265$. Note that in this case, the arc $\mathcal{A}$ varies with m, since it depends on α which varies with m. We can predict the existence and stability of the positive equilibria by the use of Theorem 3 (see Table 6).

Numerical simulations are reproduced in Fig. 6. Note that, when $0.5806 < m < 2.265$, the Poincaré-Bendixson theorem predicts that the system has at least one limit cycle that is stable in its exterior. Now, numerical simulations show that for $m = 0.5$, the system has one positive equilibrium which is LES. The unstable positive separatrix of $E_2(K, 0)$ (in green) converges towards this equilibrium, see Fig. 6 (a and b).

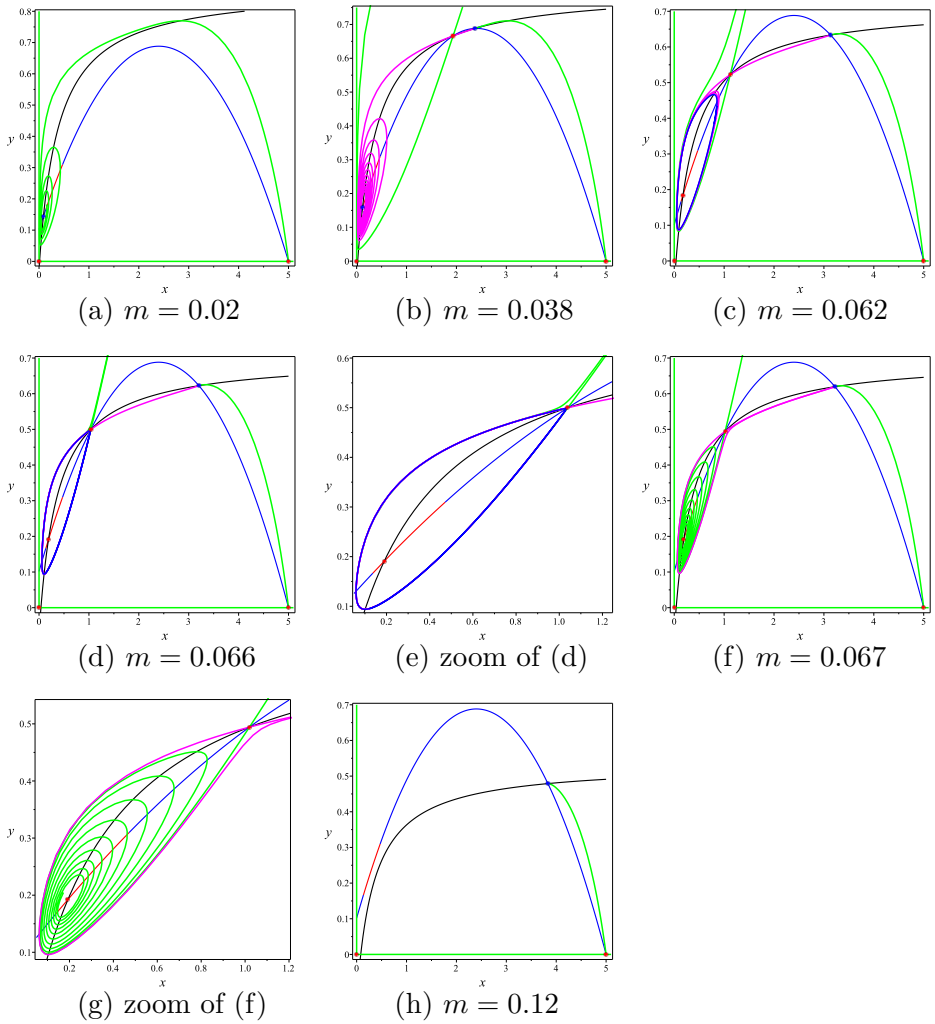

(a) $m = 0.02$ (b) $m = 0.038$ (c) $m = 0.062$

(d) $m = 0.066$ (e) zoom of (d) (f) $m = 0.067$

(g) zoom of (f) (h) $m = 0.12$

FIGURE 5. Some phase portraits of CF model with the parameter values given in Line 1 of Table 7.

TABLE 6. Positive equilibria and their stability of the CF model for the parameter values given in Line 2 of Table 7 .

m	Behavior of the system
$0 \leq m < 0.5806$	A unique positive (stable) equilibrium
$m = 0.5806$	Supercritical PAH bifurcation ($\rho = -0.3565$)
$0.5806 < m < 2.265$	A unique positive (unstable) equilibrium
$m = 2.265$	Supercritical PAH ($\rho = -0.4177$)
$2.265 < m$	A unique positive (stable) equilibrium

For $m = 1.5$, the system has one positive equilibrium which is unstable surrounded by a stable limit cycle (in blue) which has been created by a supercritical PAH bifurcation for $m = 0.5806$, see Fig. 6 (c). Note that the unstable positive separatrix of $E_2(K, 0)$ converges towards this stable limit cycle.

For $m = 2.288$, the unstable positive separatrix of $E_2(K, 0)$ converges to the unique positive LES equilibrium, see Fig. 6 (d).

For $m = 2.265$, the cycle disappears through a supercritical PAH bifurcation and not subcritical, as claimed in [6].

Here is briefly the procedure that allows us to find the bifurcation values : The PAH bifurcation values m_1 and m_2 are given by solving the equation (44) where $\alpha = \delta - m$, with respect

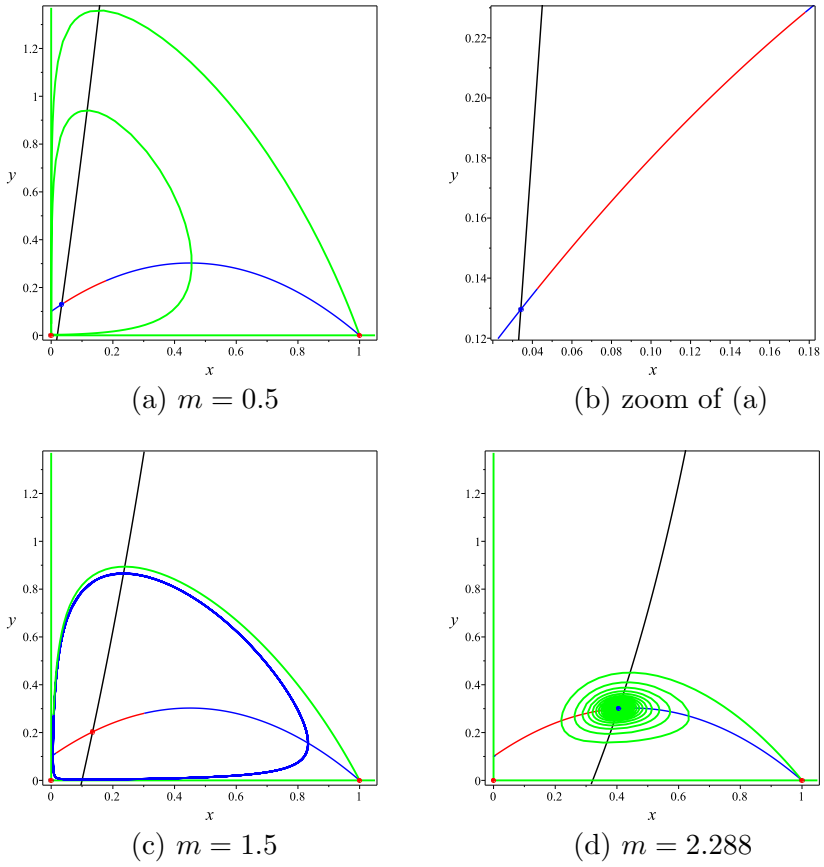

(a) $m = 0.5$ (b) zoom of (a)

(c) $m = 1.5$ (d) $m = 2.288$

FIGURE 6. Some phase portraits of CF model with the parameter values given in Line 2 of Table 7. The red arc $\mathcal{A}$ depends on m.

to m. We find a value of $m = m(x)$ that depends on x. We substitute $m(x)$ in ψ, where ψ is given in Table 1, and solve the equation $h(x) = \psi(x)$ with respect to x. We only keep the positive roots which are smaller than K, noted by x_1 and x_2. With our parameter values, we find $x_1 = 0.0390$ and $x_2 = 0.3905$. Then, by solving the equation $\psi(x_i)) = h(x_i)$, $i = 1, 2$, with respect to m, we obtain the two same values of m given in [6].

TABLE 7. The parameter values used in the CF model. The value of m is depicted on each figure.

Figure	r	K	a	c	e	α
Fig. 2(2), 5	0.28	5	0.55	0.2	0.75	0.84
Fig. 6	1	1	1	0.1	3	$2.8 - m$

4.5. **The Variable-Territory (VT) model.** In the VT model, i.e. $d(x, y) = m + \frac{\alpha y}{\delta + x}$, the system (2) is written

$$\begin{cases} \dot{x} = g(x) - yp(x), \\ \dot{y} = \left[q(x) - \frac{\alpha y}{\delta + x} - m\right] y. \end{cases} \tag{45}$$

Here again, one could write the particular form of the coefficient ρ given by (23) in the case of (45) and g, p, q given by (27). We do not do so, because of the complexity of the resulting expression. Furthermore, the equation $H(x) = G(x)$ defining the values x_L and x_R becomes now

$$\frac{ax(K - c - 2x)}{(K - x)(c + x)^2} = \frac{\alpha}{\delta + x}.$$

It is a third degree algebraic equation in x. The values x_L and x_R are the roots that lay between 0 and $\hat{x}$.

We first consider the parameter values indicated in Line 1 of Table 10. These values were chosen to reproduce, for $m = 2.4$, the case of Fig.1 (phase plot VT) in [24]. However, in [24], $\delta = 0$. To compare with this reference, and in order to use our results, we have taken a value of $\delta = 10^{-6}$ close to zero. For these parameter values, the abscissas of the ends of the arc $\mathcal{A}$, are given by $x_L = 0.2753$ and $x_R = 3.2491$, see Fig. 2(3) and Fig. 6. Note that the predator isocline passes through the ends of the arc $\mathcal{A}$ if $m = m_L = 0.7830$ and $m = m_R = 2.6888$. The first value corresponds to the passage of the predator isocline through point $(x_L, h(x_L))$, that is to say for $\tilde{x} = x_L$. The second value corresponds to the passage of the predator isocline through point $(x_R, h(x_R))$. The bifurcation values m_L and m_R are obtained by solving equation $\psi(x_i) = h(x_i)$, $i = L, R$ with respect to m.

TABLE 8. Positive equilibria and their stability of VT model for the parameter values given in Line 1 of Table 10.

m	Behavior of the system
$0 < m < 0.7830$	A unique positive (stable) equilibrium
$m = 0.7830$	Supercritical PAH bifurcation ($\rho = -0.2243$)
$0.7830 < m < 2.6888$	A unique positive (unstable) equilibrium
$m = 2.6888$	Supercritical PAH bifurcation ($\rho = -0.0097$)
$2.6888 < m$	A unique positive (stable) equilibrium

The results on the existence and stability of the positive equilibria are deduced from Theorem 3 and are summarized in Table 8. Numerical simulations are reproduced in Fig. 7. Note that when $0.7830 < m < 2.6888$, the Poincaré-Bendixson theorem predicts that the system has at least one limit cycle that is stable in its exterior.

We see numerically that for $m = 0.7$, the system has one positive equilibrium which is LES. The unstable positive separatrix of $E_2(K, 0)$ (in green) converges towards this equilibrium, see Fig. 7 (a and b).

For $m = 2.4$, the system has one positive equilibrium which is unstable surrounded by a stable limit cycle (in blue) which has been created by a supercritical PAH bifurcation for $m = 0.7830$, see Fig. 7 (c). The unstable positive separatix of $E_2(K, 0)$ converges towards this stable limit cycle.

For $m = 2.8$, the unstable separatrix of $E_2(K, 0)$ converges to the positive LES equilibrium, see Fig. 7 (d). The stable limit cycle has been destroyed through a supercritical PAH bifurcation for $m = 2.6888$.

In Fig. 8, we consider the parameter values indicated in Line 2 of Table 10. For these parameter values, the abscissas of the ends of the arc $\mathcal{A}$, are given by $x_L = 0.0065$ and $x_R = 0.9943$. Note that the predator isocline passes through the ends of the arc $\mathcal{A}$ if $m = m_L = -0.1151$ or $m = m_R = 0.2558$. The first value corresponds to the passage of the predator isocline through point $(x_L, h(x_L))$, that is to say for $\tilde{x} = x_L$. The second value corresponds to the passage of the predator isocline through point $(x_R, h(x_R))$, that is to say for $\tilde{x} = x_R$. Furthermore, the isocline of the predator is tangent to the isocline of the prey, which corresponds to a saddle-node bifurcation, when $m = 0.2518$ or $m = 0.2556$. The bifurcation values m_L and m_R are obtained by solving equation $\psi(x_i) = h(x_i)$, $i = L, R$ with respect to m.

The results on the existence and stability of the positive equilibria are deduced from Theorem 3 and are summarized in Table 9.

Note that when $m < 0.2556$ the Poincaré-Bendixson theorem predicts that the system has at least one limit cycle that is stable in its exterior. Indeed, in this case the system has only unstable equilibria. Let us illustrate the principal behaviors by numerical simulations, which will also highlight a saddle node bifurcation of cycles.

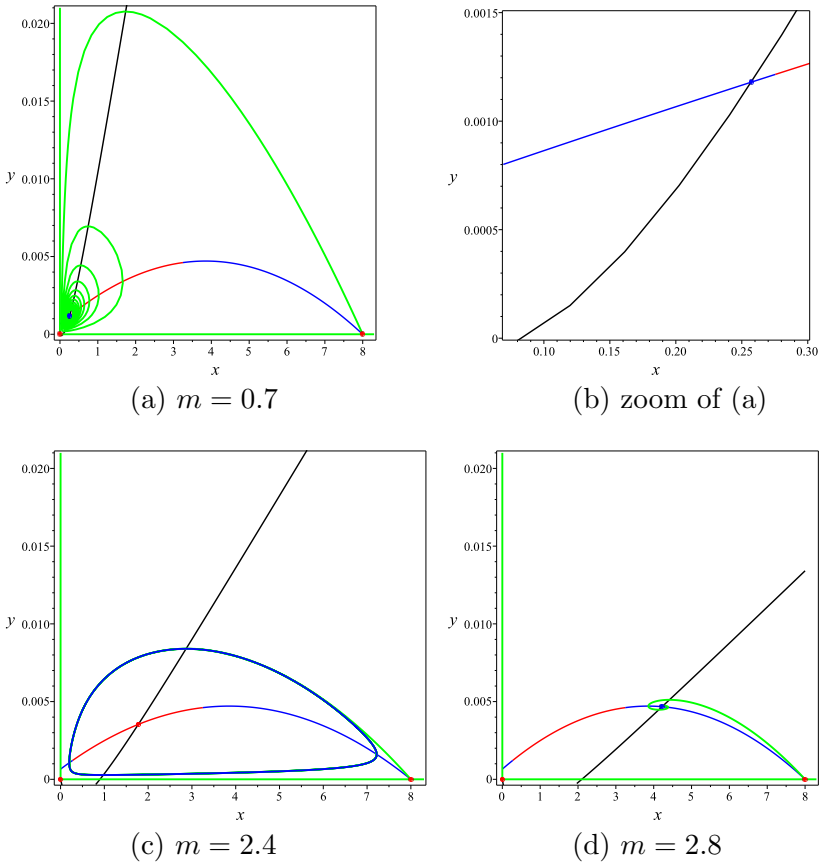

(a) $m = 0.7$ (b) zoom of (a)

(c) $m = 2.4$ (d) $m = 2.8$

FIGURE 7. Some phase portraits of VT model with the parameter values given in Line 1 of Table 10.

TABLE 9. Positive equilibria and their stability of the VT model for the parameter values given in Line 2 of Table 10.

m	Behavior of the system
$0 \leq m < 0.2518$	A unique positive (unstable) equilibrium
$m = 0.2518$	Saddle-node bifurcation
$0.2518 < m < 0.2556$	Three positive unstable equilibria
$m = 0.2556$	Saddle-node bifurcation
$0.2556 < m < 0.2558$	A unique positive (unstable) equilibrium
$m = 0.2558$	Subcritical PAH bifurcation ($\rho = 1.3839$)
$0.2558 < m$	A unique positive (stable) equilibrium

For $m = 0.1$, the system has one positive equilibrium which is unstable, surrounded by a stable limit cycle (in blue). The unstable positive separatrix of $E_2(K, 0)$ (in green) converges towards this limit cycle, see Fig. 8(a).

For $m = 0.2528$, the system has three positive equilibria. The left and the right point are unstable, the middle one is a saddle. These equilibria are surrounded by the blue stable limit cycle, see Fig. 8(b). Note that the unstable positive separatrix of $E_2(K, 0)$ and the unstable separatrices (in magenta) of the interior saddle point converge towards the limit cycle, while the stable separatrices (in green) of the interior saddle point each converge towards one of the two unstable equilibria when $t \to -\infty$. For $m = 0.2557$, the system has one positive equilibrium which is unstable, see Fig. 8(c).

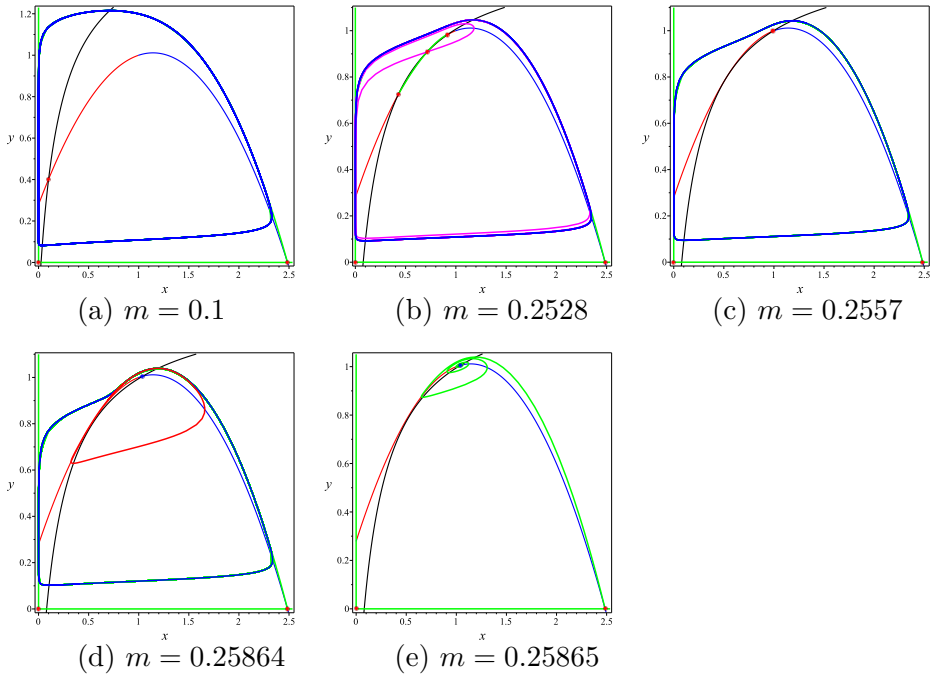

(a) $m = 0.1$ (b) $m = 0.2528$ (c) $m = 0.2557$

(d) $m = 0.25864$ (e) $m = 0.25865$

FIGURE 8. Some phase portraits of VT model with the parameter values given in Line 2 of Table 10.

For $m = 0.25864$, the system has one positive equilibrium which is LES, in addition to the big blue stable limit cycle. It is surrounded also by a small unstable limit cycle (in red) which has been created by a subcritical PAH bifurcation for $m = 0.2558$, see Fig. 8(d).

When the value of m increases, the unstable limit cycle grows and approaches the stable one. When m crosses a value between 0.25864 and 0.25865, see Fig. 8(d and e), the two limit cycles disappeared when both meat each other by a saddle node bifurcation of cycles.

For $m = 0.25167$, the system has one positive equilibrium which is LES. The unstable positive separatrix of $E_2(K, 0)$ converges towards this equilibrium.

The reader can find in [10] numerical illustrations for other sets of values of the numerical parameters of the VT model.

TABLE 10. The parameter values used for the VT model. The value of m is depicted on each figure.

Figure	r	K	a	c	e	α	δ
Fig. 2(3) and 7	1.75	8	800	0.3	0.004	169.6	10^{-6}
Fig. 8	4.97	2.4850	3.564	0.2	0.2525	40	80

5. CONCLUSION

We presented a modified Gause type model with non constant general mortality rate $d(x, y)$. We showed, under natural assumptions, that the solutions of our general model (2) are positive and bounded (Proposition 1). The system (2) always admits the boundary equilibria $E_1(0, 0)$ and $E_2(K, 0)$ and can admit positive equilibria. The necessary and sufficient condition for the existence of a positive equilibrium is $x_1 < K$, see Theorem 1. When a positive equilibrium E^* exists, the boundary equilibria E_1 and E_2 are saddle points. Moreover the determinant in E^* is positive if and only if condition (12) holds and the trace in E^* is negative if and only if condition (13) holds, see Theorem 2. The trace condition (13) is equivalent to the fact that the equilibrium E^* lies outside the subset $\mathcal{A}$ of the ascending branch of the prey isocline, see

Proposition 4. Therefore, it could be attractive even if it is located on an ascending branch of this isocline. This property never occurs for classical RMA type models for which d is constant, nor for what we called Hsu model for which $d(x, y)$ depends only on x. Geometrically, the determinant condition (12) holds if and only if, at E^*, the slope of the non trivial x-isocline is smaller than the one of the non-trivial y-isocline, see Proposition 3. In this case, E^* is LES if and only if $E^* \notin \mathcal{A}$ and is an unstable node or focus if $E^* \in int\mathcal{A}$. Finally, if condition (12) is not satisfied, E^* is a saddle point, in the hyperbolic case (Theorem 3). These geometrical observations represent an extension of the well known Rosenzweig-MacArthur criterion stability to models with variable mortality rate. We also examined the possibility of having a PAH bifurcation for the general model (2) (Theorem 4), by choosing, for sake of simplicity, the abscissa x^* of E^* as a bifurcation parameter. In particular, we were able to produce a general formula of a real number ρ corresponding to the first Lyapunov coefficient (formula (23)). If $\rho \neq 0$, the model (2) undergoes a non degenerate PAH bifurcation when x^* crosses a value $\tilde{x}$ for which the hyperbolicity and transversality conditions are verified. This bifurcation is supercritical if $\rho < 0$, and subcritical if $\rho > 0$.

We then turned our attention to some models in the literature (Table 1) : the Gause/RMA model for which the mortality rate is constant, the Hsu model with prey-dependent mortality rate, the Bazykin and CF models with predator-dependent mortality rates, and the modified VT model with predator-prey dependent mortality rate. Actually, Bazykin, CF and VT models in Table 1 are more general than their corresponding ones in the indicated references, since they are expressed using the general functions g, p and q. Our goal was the application of the results obtained for the general model which contains them all. For Gause and Hsu models, the classical Rosenzweig-MacArthur criterion of stability of a positive equilibrium holds, i.e. a positive equilibrium is LES if and only if it belongs to the decreasing branch of the prey isocline. For the others, our extension of this criterion is applicable and the closed subset $\mathcal{A}$, depending on the constant α, is a proper arc of the ascending branch of the prey isocline which tends to the whole ascending branch when α goes to zero. Hence, Theorem 3 gives us a practical reading of the local stability properties by drawing the non-trivial isoclines of the models. Furthermore, from formula (23), we choosed to deduce the expressions of the first Lyapunov coefficients for the Gause-type, Hsu and Bazykin models. For the RMA/Gause type models, we have recovered, in Proposition 5, the number ρ as given in the literature (see [28]). For the Hsu model, we were able to provide a general formula which does not seem to be known in the literature (Proposition 6). For the Bazykin model, Proposition 7 gives an original general formula of ρ. When g, p and q are given by equations (27), we have recovered the number ρ as given in [19].

Appendix A. Proof of Theorem 4.

First, by hypotheses (24) and (25) the necessary conditions (20) for a PAH Bifurcation are satisfied. Secondly, we prove the transversality condition

$$\frac{d}{dx^*} \operatorname{tr} \mathcal{J}(x^*, h(x^*))|_{x^*=\tilde{x}} \neq 0.$$

From the expression of the trace given in the proof of Theorem 2, we have

$$\operatorname{tr} \mathcal{J}(x^*, h(x^*)) = h(x^*) \left(H(x^*) - G(x^*)\right).$$

Therefore,

$$\frac{d}{dx^*} \operatorname{tr} \mathcal{J}(x^*, h(x^*)) = h'(x^*) \left(H(x^*) - G(x^*)\right) + h(x^*) \left(H'(x^*) - G'(x^*)\right).$$

By hypothesis (25), we obtain

$$\frac{d}{dx^*} \operatorname{tr} \mathcal{J}(x^*, y^*)|_{x^*=\tilde{x}} = h(\tilde{x}) \left[H'(\tilde{x}) - G'(\tilde{x})\right].$$

From the assumption (26), the transversality condition is verified. Thirdly, in order to examine the non-degeneracy condition and to compute the number ρ, the sign of which is that of the

first Lyapunov coefficient (see [12], page 169), we introduce the following change of variables

$$x = N, \quad y = h'(\tilde{x})N + \frac{\omega}{p(\tilde{x})}P, \tag{46}$$

where $\omega = \sqrt{\det \mathcal{J}(\tilde{x}, h(\tilde{x}))}$. The model (2) becomes

$$\begin{cases} \dot{N} = -\omega P + F(N,P), \\ \dot{P} = \omega N + G(N,P), \end{cases} \tag{47}$$

with

$$F(N,P) = p(N)\left[h(N) - h'(\tilde{x})N\right] - \omega P\left[\frac{p(N)}{p(\tilde{x})} - 1\right],$$

and

$$\begin{aligned} G(N,P) =& \frac{1}{\omega}\Big[q(N) - D\big(N, h'(\tilde{x})N + \frac{\omega}{p(\tilde{x})}P\big) - m\Big][p(\tilde{x})h'(\tilde{x})N + \omega P] \\ & - \frac{h'(\tilde{x})p(N)}{\omega}\Big[p(\tilde{x})h(N) - p(\tilde{x})h'(\tilde{x})N - \omega P\Big] - \omega N. \end{aligned}$$

The parameter ρ is given by

$$\rho = \frac{1}{16}A_1 + \frac{1}{16\omega}\left[A_2 - A_3 - A_4\right], \tag{48}$$

where, see [12], page 169 or [8], page 152

$$A_1 = F_{NNN} + F_{NPP} + G_{NNP} + G_{PPP}, \quad A_2 = F_{NP}(F_{NN} + F_{PP}),$$

$$A_3 = G_{NP}(G_{NN} + G_{PP}), \quad A_4 = F_{NN}G_{NN} - F_{PP}G_{PP}.$$

where F_{NN} denotes $\frac{\partial^2 F}{\partial N \partial N}(\tilde{N}, \tilde{P})$, F_{NP} denotes $\frac{\partial^2 F}{\partial N \partial P}(\tilde{N}, \tilde{P})$, and similarly for all other partial derivatives. Since F is linear in P, we have $F_{PP} = F_{NPP} = 0$. Notice that from the change of variables (46), we have $\tilde{N} = \tilde{x}$ and $\tilde{P} = \frac{p(\tilde{x})}{\omega}\left(\tilde{y} - h'\left(\tilde{x}\right)\tilde{x}\right)$.

After calculations, and using the notations (21), we find that A_i, $i = 1, \cdots, 4$ are given by the following expressions

$$\begin{aligned} A_1 =& \frac{1}{p_0^2}\Big[p_0^2p_2h_1 + 3p_0^2p_1h_2 + p_0^3h_3 + p_0^2q_2 - p_0^2d_{11} - 4p_0^2h_1d_{12} - 3\left(\omega^2 + p_0^2h_1^2\right)d_{22} \\ & - p_0^2h_0d_{112} - \left(\omega^2 + p_0^2h_1^2\right)h_0d_{222} - 2p_0^2h_0h_1d_{122}\Big], \\ A_2 =& -\omega p_1h_2, \\ A_3 =& \frac{1}{p_0\omega}\Big[p_1h_1 + q_1 - d_1 - 2h_1d_2 - h_0d_{12} - h_0h_1d_{22}\Big]\Big[p_0^2q_2h_0 - p_0^3h_1h_2 + 2p_0^2q_1h_1 \\ & - 2p_0^2h_1d_1 - 2\left(\omega^2 + p_0^2h_1^2\right)d_2 - p_0^2h_0d_{11} - 2p_0^2h_0h_1d_{12} - \left(\omega^2 + p_0^2h_1^2\right)h_0d_{22}\Big], \\ A_4 =& \frac{p_0^2h_2}{\omega}\Big[q_2h_0 - p_0h_1h_2 + 2q_1h_1 - 2h_1d_1 - 2h_1^2d_2 - h_0d_{11} - 2h_0h_1d_{12} - h_0h_1^2d_{22}\Big]. \end{aligned}$$

Replacing these expressions in (48) we obtain the following formula for ρ

$$\rho = \frac{1}{16p_0^2\omega^2}\left(a_0 + a_2\omega^2 + a_4\omega^4\right),$$

where a_0, a_2 and a_4 do not depend on ω. Using MAPLE [20] now, we can replace ω^2 by its expression (22) and h_1 by $h_1 = d_2h_0/p_0$, which follows from the condition $H(\tilde{x}) = G(\tilde{x})$. We obtain the expression of ρ given by (23).

Under the assumption that $\rho \neq 0$ we conclude that (2) undergoes a non degenerate PAH bifurcation at $\tilde{E}(\tilde{x}, \tilde{y})$, see Theorem 3.4.2 in [8].

Appendix B. Biological explanations

It is not useless to give briefly some biological explanations for the models we used to illustrate our results (see for example Table 1 in [25]). In RMA and Gause models, the prey density is regulated only by food limitation ($d(x, y) = m$). In the Hsu model, the mortality rate is a decreasing function of the prey density. In [11], Hsu indicates for example the case $d(x) = (ex+f)/(rx+s)$ with $fe > se$ which can be written in the form $m+\alpha/(\delta+x)$. In this reference, there is no justification for this rate. However, it can be interpreted naturally by the fact that the more the prey is available, the more the predator mortality rate is small. May be a better justification is to consider $d(x)y$ as an emigration term, in the sense that predators get out of the ecosystem when the density of the prey is small. The Hsu model contains also a model due to Minter et al. [21] where a detailed biological justification leads to a mortality rate of the form $d(x) = \alpha/(\delta + x)$ for which $d(x)$ decreases to zero when x goes to infinity. Bazykin [2, 3, 19] introduced the regulation by interspecific mechanisms, that is a competition among predators for resources other than prey. To do this, he subtracted a quantity αy^2 from the predator equation ($d(x, y) = m+\alpha y$). Even if not concerned by our study, it is also worth mentioning the recent article [14] which deals with Bazykin model with ratio-dependent functional response of Arditi-Ginzburg. If the predator density-dependence parameter α is made inversely proportional to resource availability, the dynamics are described by the variable-territory model of Turchin-Batzli [24, 25] ($d(x, y) = m+\alpha y/x$, where α is called the prey/predator ratio at equilibrium). The term $d(x, y)y = \alpha y^2/x$ in the predator equation represents the self-limitation of the predator. Nevertheless, a self-limitation should be biologically limited. It is not the case for Turchin-Batzli model where $\alpha y^2/x$ could become quite large in case of predators can subsist on few prey (i.e. $\alpha y^2/x \to \infty$ as $x \to 0$). This leads to the well-defined modified VT model for which $d(x, y) = m + \frac{\alpha y}{\delta+x}$ where $\delta > 0$ is fixed [13]. Not only the self limitation of predator becomes less than $\alpha y^2/d$ but also the singularity in $x = 0$ is avoided. Cavani and Farkas [5, 6] proposed the modified RMA model for which the mortality of the predator in the absence of the prey is a growing and bounded function of the predator quantity. More exactly $d(x, y) = m + \alpha y/(1 + y)$ where, contrary to what we assumed for technical reasons, $\alpha = \delta - m$ depends on m. Here, $m > 0$ is the mortality at low density and is less than δ which is the limiting, maximal mortality. Except for Gause, Hsu and Bazykin models, the theoretical study of these models is not, for our knowledge, always exhaustive. Authors have sometimes directed their investigation to a particular aspect, especially the appearance of periodic orbits. Indeed, all the mentioned models can generically exhibit limit cycles that can appear or disappear by PAH bifurcation.

Acknowledgments

The authors thank the Algerian-Tunisian research project: Mathematical ecology, modeling and optimization of depollution bioprocesses and the Euro-Mediterranean research network TREASURE (`http://www.inrae.fr/treasure`).

References

[1] R. Arditi and L. Ginzburg, Coupling in predator-prey dynamics: Ratio-dependence, *Journal of Theoretical Biology* 139 (1989) 311–326. `https://doi.org/10.1016/s0022-5193(89)80211-5`

[2] A. D. Bazykin, Volterra's system and the Michaelis-Menten equation, *Problems in mathematical genetics. USSR Academy of Science, Novosibirsk, USSR* (1974) 103–142.

[3] A. D. Bazykin Nonlinear dynamics of interacting populations, *World Scientific (1998).* `https://doi.org/10.1142/2284`

[4] N. Beroual and T. Sari A predator-prey system with Holling-type functional response *Proc. Amer. Math. Soc.* 148 (2020), 5127-5140. `https://doi.org/10.1090/proc/15166`

[5] M. Cavani and M. Farkas Bifurcations in a predator-prey model with memory and diffusion I: Andronov-Hopf bifurcation, *Acta Mathematica Hungarica*, 63 (1994) 213–229. `https://doi.org/10.1007/bf01874129`

[6] C. Duque and M. Lizana, Partial characterization of the global dynamic of a predator-prey model with non constant mortality rate, *Differential Equations and Dynamical Systems*, 17 (2009) 63–75 `https://doi.org/10.1007/s12591-009-0005-y`

[7] H. I. Freedman, Deterministic Mathematical Models in Population Ecology, Volume 57 of Monographs and textbooks in pure and applied mathematics, M. Dekker (1980).

[8] J. Guckenheimer and P. Holmes, Nonlinear Oscillations, Dynamical Systems, and Bifurcations of Vector Fields, Springer-Verlag (2002). https://doi.org/10.1007/978-1-4612-1140-2
[9] J. Hainzl, Stability and Hopf Bifurcation in a Predator-Prey System with Several Parameters, *SIAM Journal on Applied Mathematics*, 48 (1988) 170–190. https://doi.org/10.1137/0148008
[10] A. Hammoum, T. Sari and K. Yadi, Rosenzweig-MacArthur model with variable disappearance rate. *CARI'2022, Proceedings of the 16th African Conference on Research in Computer Science and Applied Mathematics*, (2022). https://hal.inria.fr/CARI2022/hal-03712243
[11] S.B. Hsu, On Global Stability of a Predator-Prey System, *Mathematical Biosciences*, **39** (1978) 1–10. https://doi.org/10.1016/0025-5564(78)90025-1
[12] E. M. Izhikevich Dynamical systems in neuroscience, MIT press (2007). https://doi.org/10.7551/mitpress/2526.001.0001
[13] H. Jiang and L. Wang, Analysis of Steady State for Variable-Territory Model with Limited Self-Limitation, *Acta Applicandae Mathematicae*, 148 (2017) 103–120. https://doi.org/10.1007/s10440-016-0080-3
[14] X. Jiang, Z. She and S. Ruan, Global dynamics of a predator-prey system with density-dependent mortality and ratio-dependent functional response, *Discrete & Continuous Dynamical Systems-B*, 26 (2021) 1967–1990. http://dx.doi.org/10.3934/dcdsb.2020041
[15] A. Kolmogorov, Sulla teoria di Volterra della lotta per lesistenza, *Gi. Inst. Ital. Attuari*, 7 (1936) 74–80.
[16] M. Kot, Elements of mathematical ecology, Cambridge University Press (2001). https://doi.org/10.1017/CBO9780511608520
[17] Y.A. Kuznetsov, Elements of Applied Bifurcation Theory, Applied Mathematical Sciences (AMS, volume 112), Springer New York, NY (2004). https://doi.org/10.1007/978-1-4757-3978-7
[18] C. Lobry, The Consumer-Resource Relationship: Mathematical Modeling, Wiley-ISTE (2018). https://doi.org/10.1002/9781119544029
[19] M. Lu and J. Huang, Global analysis in Bazykin's model with Holling II functional response and predator competition, *Journal of Differential Equations*, 280 (2021) 99–138. https://doi.org/10.1016/j.jde.2021.01.025
[20] MAPLE [Software], Version 13.0, *Maplesoft*, a division of Waterloo Maple Inc., Waterloo, Ontario (2009). https://fr.maplesoft.com/
[21] E. J. Minter, A. Fenton, J. Cooper and D. J. Montagnes, Prey-dependent mortality rate: a critical parameter in microbial models, *Microbial ecology*, 62 (2011) 155-161. https://doi.org/10.1007/s00248-011-9836-5
[22] M. L. Rosenzweig and R. H. MacArthur, Graphical representation and stability conditions of predator-prey interaction, *Amer. Natur.* 47 (1963) 209-223. https://doi.org/10.1086/282272
[23] G. Seo and G. S. K. Wolkowicz, Sensitivity of the dynamics of the general Rosenzweig–MacArthur model to the mathematical form of the functional response: a bifurcation theory approach, *Journal of Mathematical Biology*, 76 (2018) 1873–1906. https://doi.org/10.1007/s00285-017-1201-y
[24] S. Strohm and R. Tyson, The effect of habitat fragmentation on cyclic population dynamics: a numerical study, *Bulletin of Mathematical Biology*, 71 (2009) 1323–1348. https://doi.org/10.1007/s11538-009-9403-0
[25] P. Turchin and G. O. Batzli, Availability of food and the population dynamics of arvicoline rodents, *Ecology*, 82 (2001) 1521–1534. https://doi.org/10.1890/0012-9658(2001)082[1521:aofatp]2.0.co;2
[26] V. Volterra, Variazioni e fluttuazioni del numero di individui in specie animali conviventi, *Atti Reale Accad. Nazionale dei Lincei*, 6 (1927) 641–648.
[27] S. Wang and H. Yu, Stability and bifurcation analysis of the Bazykin's predator-prey ecosystem with Holling type II functional response, *Math. Biosci. Engin*, 18 (2021) 7877–7918. https://doi.org/10.3934/mbe.2021391
[28] G. S. K. Wolkowicz, Bifurcation analysis of a predator-prey system involving group defence, *SIAM Journal on Applied Mathematics*, 48 (1988) 592–606. https://doi.org/10.1137/0148033

LSDA, University Abou Bekr Belkaid, Tlemcen, Algeria
Email address: amina.hammoum@univ-tlemcen.dz

ITAP, Univ Montpellier, INRAE, Institut Agro, Montpellier, France
Email address: Tewfik.Sari@inrae.fr

LSDA, University Abou Bekr Belkaid, Tlemcen, Algeria
Email address: karim.yadi@univ-tlemcen.dz